

2021-05-21

# Hardground, gap and thin black shale: spatial heterogeneity of arrested carbonate sedimentation during the Jenkyns Event (T-OAE) in a Tethyan pelagic Basin (Gerecse Mts, Hungary)

Muller, T

<http://hdl.handle.net/10026.1/18392>

---

10.1144/sp514-2020-266

Geological Society, London, Special Publications

Geological Society of London

---

*All content in PEARL is protected by copyright law. Author manuscripts are made available in accordance with publisher policies. Please cite only the published version using the details provided on the item record or document. In the absence of an open licence (e.g. Creative Commons), permissions for further reuse of content should be sought from the publisher or author.*

# Hardground, gap and thin black shale: spatial heterogeneity of arrested carbonate sedimentation during the Jenkyns Event (T-OAE) in a Tethyan pelagic Basin (Gerecse Mts, Hungary)

Tamás Müller<sup>1,2\*</sup>, Gregory D. Price<sup>3</sup>, Emanuela Mattioli<sup>4,5</sup>, Máté Zs. Leskó<sup>6</sup>, Ferenc Kristály<sup>6</sup> and József Pálffy<sup>2,7</sup>

<sup>1</sup>Isotope Climatology and Environmental Research Centre, Institute for Nuclear Research,

Bem tér 18/C, H-4026, Debrecen, Hungary

<sup>2</sup>Department of Geology, Eötvös Loránd University, Pázmány Péter sétány 1/C, Budapest

H-1117, Hungary

<sup>3</sup>School of Geography, Earth and Environmental Sciences, Plymouth University, Drake Circus, Plymouth, PL4 8AA, UK

<sup>4</sup>Univ Lyon1, ENSL, CNRS, LGL-TPE, F-69622, Villeurbanne, France <sup>5</sup>Institut Universitaire de France, Paris, France

<sup>6</sup>Institute of Mineralogy and Geology, University of Miskolc, HU-3515 Miskolc-Egyetemváros, Miskolc, Hungary

<sup>7</sup>MTA-MTM-ELTE Research Group for Paleontology, POB 137, H-1431, Budapest, Hungary

**Abstract:** The Jenkyns Event or Toarcian Oceanic Anoxic Event was an episode of severe environmental perturbations reflected in carbon isotope and other geochemical anomalies. Although well studied in the epicontinental basins in NW Europe, its effects are less understood in open marine environments. Here we present new geochemical (carbon isotope, CaCO<sub>3</sub>, [Mn]) and nannofossil biostratigraphic data from the Tölgyhát and Kisgerecse sections in the Gerecse Hills (Hungary). These sections record pelagic carbonate sedimentation near the margin of the Tethys Ocean. A negative carbon isotope excursion of c. 6‰ is observed in the Tölgyhát section, in a condensed clay and black shale layer where the CaCO<sub>3</sub> content drops in association with the Jenkyns Event. At Kisgerecse, bio- and chemostratigraphic data suggest a gap in the lower Toarcian. The presence of an uppermost Pliensbachian hardground, the absence of the lowermost Toarcian *Tenuicostatum ammonite* zone and the condensed record of the Jenkyns Event at Tölgyhát, together with a condensed *Tenuicostatum* Zone and the missing negative carbon isotope anomaly at Kisgerecse, imply arrested carbonate sedimentation. A calcification crisis and sea-level rise together led to a decrease in carbonate production and terrigenous input, suggesting that volcanogenic CO<sub>2</sub>-driven global warming may have been their common cause. Supplementary material: Geochemical data obtained from Tölgyhát and Kisgerecse sections, and mineralogical data from Tölgyhát are available at <https://doi.org/10.6084/m9.figshare.c.5355342>

In the Early Jurassic, a series of severe environmental perturbations such as global warming (Suan et al. 2010), a second-order mass extinction (Caruthers et al. 2014), ocean anoxia (Pearce et al. 2008) and a calcification crisis (Trecalli et al. 2012) happened in the early Toarcian (c. 183 Ma), collectively referred to as Toarcian Oceanic Anoxic Event (T-OAE) (Jenkyns 1988; Jenkyns 2010) or recently coined as the Jenkyns Event (Müller et al. 2017; Reolid et al. 2020). This time interval was characterized by enhanced marine primary production leading to the appearance of organic-rich sediments in marine and lacustrine settings under anoxic–euxinic conditions (Jenkyns 1988; Xu et al. 2017). However, some other authors point to a high primary production occurring before the event and to a phytoplankton blackout concomitant with it (Bucefalo Palliani et al. 2002; Mattioli et al. 2009). The Jenkyns Event is coincident with a characteristic negative carbon isotope excursion (CIE) with a magnitude of c. 5‰ (Hesselbo et al. 2000; Hermoso et al. 2009; Suan et al. 2015). This negative CIE is present in different substrates, e.g. marine biogenic carbonate and micrite, and in marine and terrestrial organic matter, implying a major perturbation of the carbon cycle affecting the exogenic carbon reservoirs (Suan et al. 2008a; Hermoso et al. 2009; Bodin et al. 2010; Suan et al. 2010; Hesselbo and Pieńkowski 2011; Müller et al. 2020b). Furthermore, this carbon isotope anomaly can be also traced at multiple localities around the world, suggesting a global extent of this event (Caruthers et al. 2011; Gröcke et al. 2011; Suan et al. 2011; Izumi et al. 2012; Al-Suwaidi et al. 2016). A second-order mass extinction is also associated with the Jenkyns Event severely affecting the biosphere (Caswell et al. 2009; Danise et al. 2013; Caruthers et al. 2014), with a remarkable temporal coincidence with the emplacements of the Karoo–Ferrar large igneous province (LIP) (Pálffy and Smith 2000). The large amount of <sup>12</sup>C that triggered the negative CIE has been hypothesized to have originated from volcanic degassing of CO<sub>2</sub> from the Karoo–Ferrar LIP and/or thermogenic methane release from coal sediments in the Karoo Basin owing to sill emplacements (McElwain et al. 2005; Svensen et al. 2007). Alternatively, methanehydrate dissociation from marine sediments (Hesselbo et al. 2000; Kemp et al. 2005), methane release from terrestrial wetlands and/or from permafrost (Them et al. 2017; Krencker et al. 2019; Ruebsam et al. 2019) and upwelling of <sup>12</sup>C-rich bottom water and stratification of the water column (Küspert 1982; Schouten et al. 2000) have been suggested as causes. The negative CIE and CO<sub>2</sub> release are also coincident with global warming and a rapid temperature rise of c. 7°C (Bailey et al. 2003; Suan et al. 2010). The globally elevated temperature resulted in the acceleration of the hydrological cycle, increased continental runoff and nutrient input into the ocean, further increasing primary productivity (Cohen et al. 2004; Jenkyns 2010; Percival et al. 2016; Kemp et al. 2020). This high primary productivity led to oxygen depletion of the seawater, resulting in the development of anoxic or euxinic water masses, occasionally even spreading to the photic

zone (van de Schootbrugge et al. 2005; Pearce et al. 2008; Ruebsam et al. 2018). Thallium isotope studies revealed that seawater oxygen levels had started to drop gradually at the Pliensbachian/Toarcian boundary and reached euxinic conditions during the Jenkyns Event (Them et al. 2018). This is coherent with enhanced primary productivity occurring from the base of the Toarcian, followed by enhanced thermohaline stratification promoting anoxia at the core of the event (Bucefalo Palliani et al. 2002; Mattioli et al. 2009). A biocalcification crisis simultaneous with the Jenkyns Event severely affected both carbonate platforms and pelagic carbonate factories (Mattioli et al. 2009; Trecalli et al. 2012; Krencker et al. 2020; Müller et al. 2020b; Ettinger et al. 2021). Brachiopod  $\delta^{11}\text{B}$ -pH data imply that seawater pH started to drop in multiple steps immediately after the Pliensbachian/Toarcian boundary, reaching the minimum (c. 7.2; a total drop of 0.4–0.5 in pH values) immediately before and during the Jenkyns Event, which suggests a significant global lowering of seawater pH. A remarkable, rapid rise in pH at the onset of the Jenkyns Event indicates that organic carbon production and burial increased the withdrawal of atmospheric  $\text{CO}_2$  simultaneously with the start of the negative CIE. Carbonate system modelling revealed that the pH decrease was also accompanied by a substantial drop in seawater carbonate saturation ( $\Omega_1$ ) (Müller et al. 2020a).

In order to better assess the global extent of this chain of environmental perturbations related to the Jenkyns Event oceanic records would be necessary but little oceanic crust of Toarcian age is preserved. Therefore, pelagic successions with a depositional setting close to the open ocean have key importance (Suan et al. 2018). So far, only a handful of such sections have been studied from the sedimentary record of the Panthalassan margin in Japan and Canada (Caruthers et al. 2011; Gröcke et al. 2011) and from the NW Tethyan margin from European sections (Jenkyns et al. 1991; Vető et al. 1997; Kafousia et al. 2011; Neumeister et al. 2015; Polgári et al. 2016; Arabas et al. 2017; Müller et al. 2017, 2020b; Suan et al. 2018).

To augment this dataset and to improve our understanding of the local and regional differences in the processes and expression of the Jenkyns Event, here we present new high-resolution carbon isotope,  $\text{CaCO}_3$  and [Mn] geochemical data, nannofossil biostratigraphy and mineralogical information from two sections, Tölgyhát and Kisgerecse, from the Gerecse Hills in north-central Hungary. These sections are biostratigraphically well constrained (Géczy 1984, 1985; Kovács 2012) and exhibit lithological variations that reflect the early Toarcian environmental and biotic changes. Palaeogeographically, they represent condensed, pelagic records of the early Toarcian in an ocean-facing setting with proximity to the open Tethys Ocean (Fig. 1). Our study aims to characterize the changes in pelagic carbonate sedimentation and their relation to a possible ocean acidification and calcification crisis that, compared with the extent and effects of anoxia, is a lesser known component of the Jenkyns Event.

### Geological background and stratigraphy

The Gerecse Hills are located in north-central Hungary, 50 km NW of Budapest, in the northeastern part of the Transdanubian Range (Fig. 2a). In the Late Triassic, this area was located at the margin of the Tethys Ocean where the depositional environment was dominated by the extensive Dachstein carbonate platform. Regional rifting started in the latest Triassic and earliest Jurassic and later, in the Middle Jurassic, led to the opening of the Penninic Ocean. As a result, the platform was dissected and differential subsidence throughout the Early Jurassic created a depositional environment with small local basins and intervening elevated submarine highs (Császár et al. 1998). The Hettangian strata in the Gerecse Hills are assigned to the Pisznice Limestone Fm. The lower part of this unit is pink, thick-bedded limestone (Fig. 2b, c) that contains intraclasts and bioclasts including brachiopods and crinoids, suggesting a high-energy, shallow marine depositional environment. The upper part of the Pisznice Fm. is Sinemurian–early Pliensbachian in age and consists of more thinly bedded, red nodular pelagic limestones of ammonitico rosso facies with a rich brachiopod fauna (Dulai 1998; Császár et al. 1998). The thickness of the Pisznice Fm. varies locally between 20 and 55 m and reflects the articulated palaeotopography. Another Sinemurian formation in the Gerecse is the Hierlatz Limestone Fm. that appears as crinoid- and brachiopod-rich talus breccia or infill of neptunian dykes in older formations (i.e. (a)(b) the Dachstein Limestone and the Pisznice Limestone). The upper part of the Pliensbachian belongs to the Törökbükk Limestone Fm. that does not exceed a few metres in thickness and shows similar facies and depositional conditions to the Pisznice Fm. but contains abundant manganiferous nodules and intraclasts with Mn coating and is locally crinoidal (Császár et al. 1998; Sasvári et al. 2009; Budai et al. 2018). Alternatively, this unit was assigned to the Tűzkövesárok Fm. that is also characterized by ammonitico rosso-type lithofacies but is more widespread further west in the Transdanubian Range, in the Bakony Mts. The late Pliensbachian ammonite *Fucineras* was reported from this unit from the intensively studied section at Tata (Fülöp 1976).

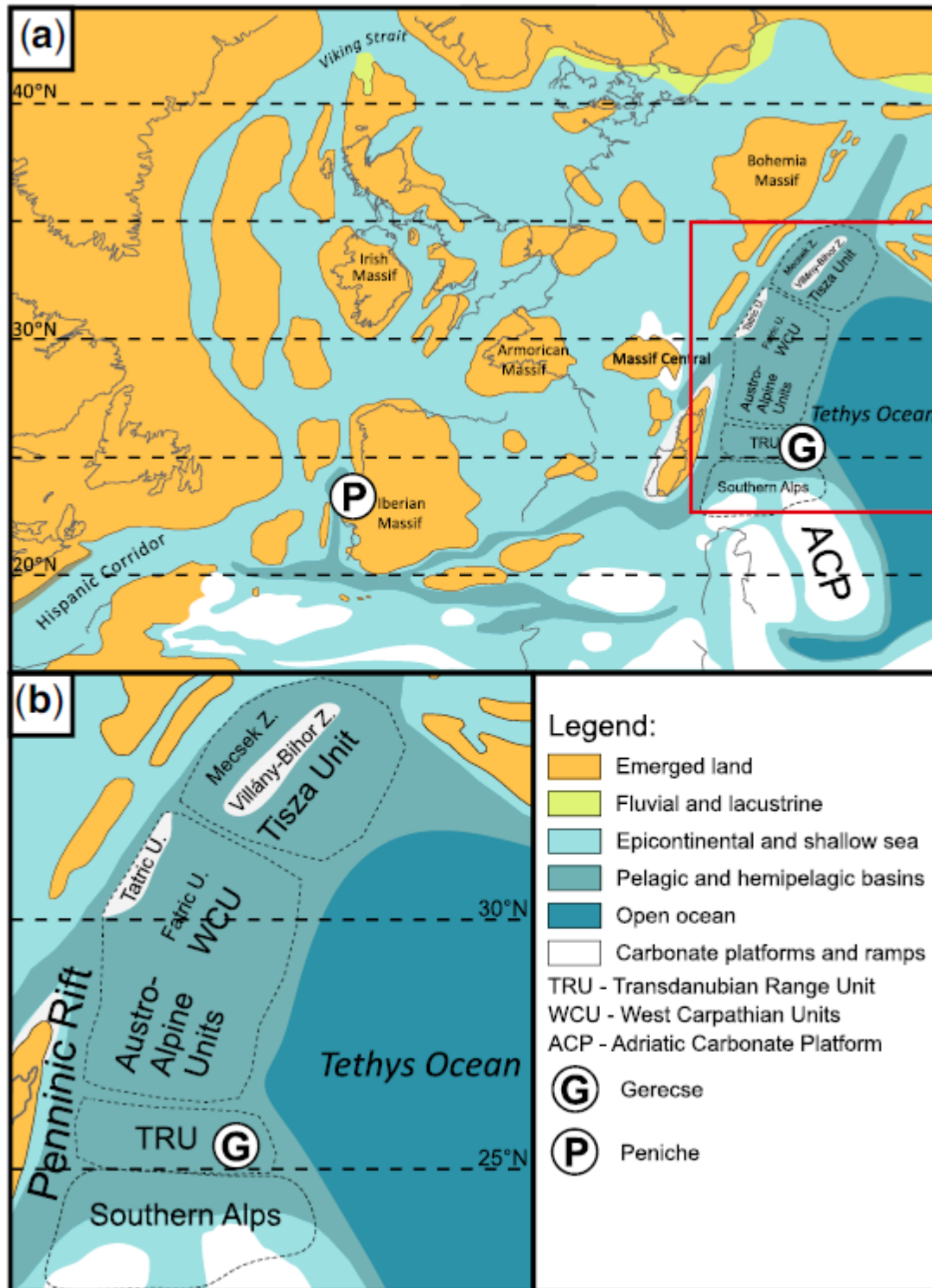


Fig. 1. (a) Palaeogeographic map of Europe and the NW Tethys during the Early Jurassic (modified from Thierry and Barrier 2000). Supposed positions of the NW Tethyan tectonic units (TRU, Transdanubian Range Unit, Austro-Alpine Units; WCU, Western Carpathian Units and Tisza Unit) are marked with dashed line. Modified from Häusler et al. (1993) and Haas (2012). (b) Close-up view of the NW Tethyan margin during the Early Jurassic.

The Pliensbachian–Toarcian boundary is commonly marked by an uneven, 1–2 cm thick Fe–Mn-bearing hardground or a distinct sedimentary gap at different localities. In the Bakony Mts, the Úrkút Manganese Ore Fm. forms a c. 40 m thick, economically significant manganese ore deposit with organic-rich black shale intercalations. This unit is considered to represent the Jenkyns Event, expressed in peculiar, temporally and

spatially restricted ore-forming processes (Haas 2012; Polgári et al. 2016; Suan et al. 2016). In the Gerecse Hills

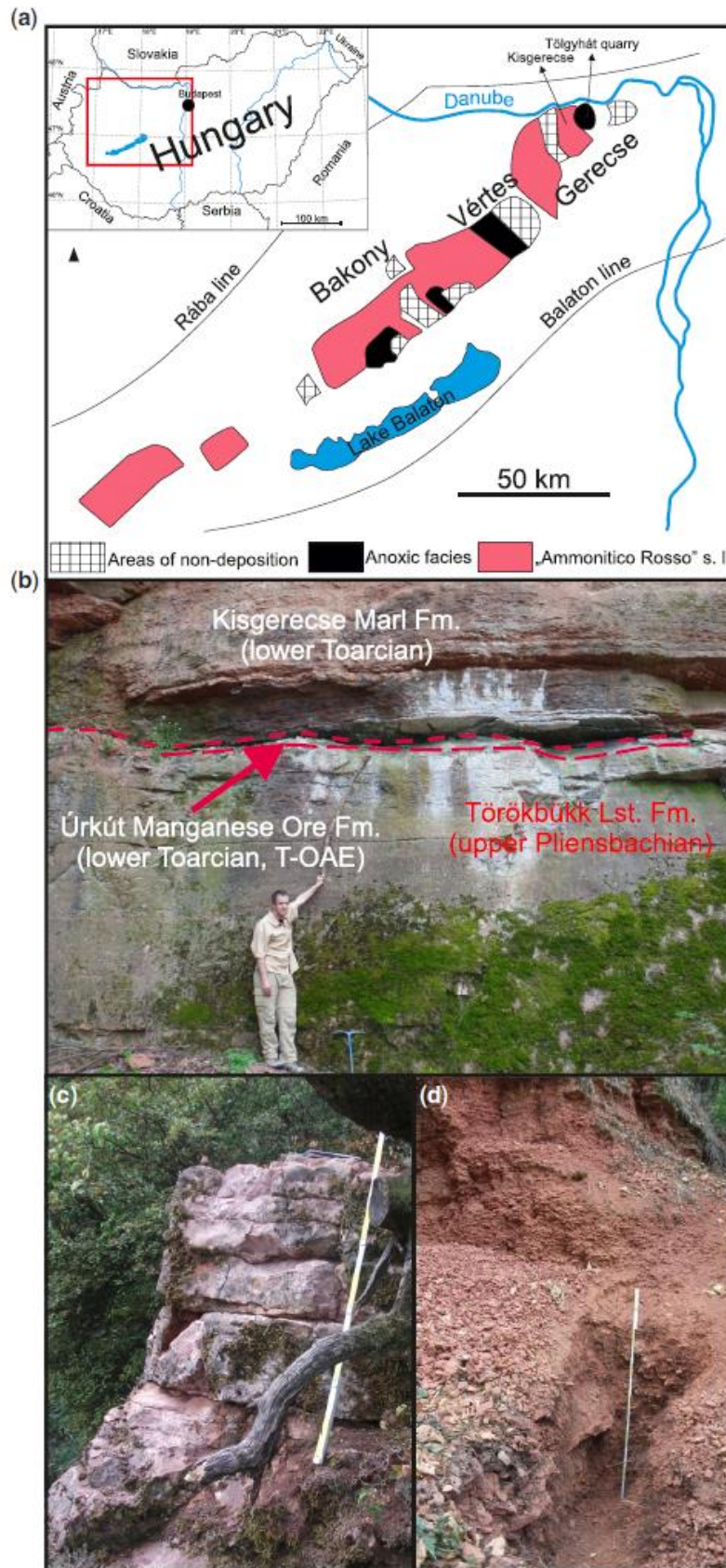


Fig. 2. (a) Locations of the studied sections and map of sedimentary facies of the Toarcian deposits in the Transdanubian Range (after Vörös and Galács 1998). (b) Upper Pliensbachian and lower Toarcian pelagic succession exposed in an abandoned quarry at Tölgyhát. (c) Uppermost Pliensbachian beds of the Törökbükk Fm. from the Kisgerecse section. (d) Trench exploring the lower Toarcian Kisgerecse Fm. at the Kisgerecse section



the Úrkút Fm. is only present in the Tölgyhát quarry section, where it is limited to a 10–30 cm thick bed (Fig. 2b; Konda 1988; Sasvári et al. 2009). Although ammonites do not occur in the Úrkút Fm. in the Gerecse Hills, on the basis of facies similarities with the Úrkút locality an early Toarcian age, equivalent to that of the Tenuicostatum and Serpentinum zones, is assumed (Császár et al. 1998). From the Úrkút Fm. at the Tölgyhát Quarry, Polgári et al. (2000) reported a single total organic carbon measurement of 2.68 wt%. This unit is locally divided into two lithofacies. The lower half is a yellowish, thin layered clayey marl with manganese nodules, whereas the upper half is a thin-layered organic-rich black shale. Above this unit and elsewhere in the Gerecse Hills the lower Toarcian is represented by the c. 3 m thick Kisgerecse Marl Fm. This formation consists of thin-bedded red nodular pelagic marl and marly limestone (Fig. 2b, d) with a rich ammonoid fauna that indicates the presence of the Serpentinum and Bifrons zones, proven in the studied sections by the occurrence of subzonal index taxa *Harpoceras serpentinum*, *H. falciferum* and *Hildoceras sublevisoni* (Géczy 1985; Kovács 2012). At only one locality, in the Kisgerecse section, a single 5 cm thick limestone layer immediately overlying the top of the Pliensbachian Törökbükk Fm. yielded *Fontanelliceras* cf. *fontanellense*. This ammonoid species was considered diagnostic of the Tenuicostatum Zone (Géczy 1984, 1985; Kovács 2012), but it is now thought to have a narrow range straddling the Pliensbachian/Toarcian boundary, from the upper Emaciatum/Spinatum to lowermost Tenuicostatum zones (Meister et al. 2017). Nevertheless, with the possible exception of the Kisgerecse locality, the Tenuicostatum Zone has not been identified in any other section in the Gerecse Hills, and Toarcian successions commonly start in the Serpentinum Zone (Kovács 2012), indicative of a hiatus. A detailed biostratigraphic study at nearby Nagy–Pisznice Hill documented that the upper part of the Kisgerecse Fm. belongs to the Gradatus Zone and the topmost bed of the formation represents the base of the overlying late Toarcian Thouarsense Zone, revealed by the occurrence of zonal index species *Merlaites gradatus* and *Grammoceras thouarsense*, respectively (Galács et al. 2010). On top of the Kisgerecse Fm. after a distinct albeit gradual facies shift, deposition of the red nodular, ammonitico rosso-type pelagic limestone returns with some marly intercalations in the Tölgyhát Limestone Fm. that continues up to the Bajocian (Császár et al. 1998; Budai et al. 2018). The relationships of these Jurassic lithostratigraphic units of the study area in the Gerecse and adjacent parts of the Transdanubian Range are summarized in Figure 3. In this study we have investigated a 2.2 m interval in the Tölgyhát Quarry section (Figs 2b and 4) (47°43' 22.0" N; 18°30' 46.7" E), covering the uppermost Pliensbachian part of the Törökbükk Fm., the 24 cm thick Úrkút Fm. separated by a 1–5 cm thick hardground from the underlying Törökbükk Fm. and the lower part of the Kisgerecse Fm. that reaches up to the middle Toarcian Bifrons Zone. The Tölgyhát quarry exposes the most complete and expanded Jurassic section that is thought to represent a local basinal setting (Budai et al. 2018). In addition, a 2.3 m thick interval section excavated above the Kisgerecse quarry (Figs 2c, d and 5; 47°41' 22.6" N; 18°29' 36.8" E) was investigated, covering the uppermost c. 30 cm of the Törökbükk Fm. and the lower c. 2 m of the Kisgerecse Fm., reaching the Bifrons Zone as well. Short accounts of these two sections, only 4 km apart, were provided by Konda (1986, 1988), whereas detailed stratigraphic results of a recently completed geological mapping project are found in Budai et al. (2018).

## Methods

At both the Tölgyhát and Kisgerecse sections high-resolution sampling was carried out after detailed measurements of the target intervals of 2.2 and 2.3 m thickness, respectively. A cordless drill with hardened steel drill bit was used to obtain rock powder for carbon and oxygen isotope ratio measurements and major- and minor-element inductively coupled plasma atomic emission spectrometry (ICP-AES) analyses. A total of 58 samples were collected from the Tölgyhát and 49 from the Kisgerecse sections. Sample spacing was 2 cm at the lowermost 1 m of the sections and 10 cm higher up. In addition, during a subsequent sampling campaign, 17 bulk samples were collected from the Tölgyhát section for mineral composition and X-ray powder diffraction (XRD) analyses, covering the interval between c. 0.3 and 1.3 m. In order to improve the biostratigraphic control, 18 bulk rock samples were taken from the Tölgyhát section for nannofossil analyses. Carbon and oxygen isotope and ICP-AES elemental analyses were carried out at the geochemical laboratory of the University of Plymouth (UK). Samples of 200–500 µg of carbonate were reacted with 100% phosphoric acid and stable isotope data were generated on a VG Optima mass spectrometer with a Gilson autosampler. Carbon and oxygen isotope ratios are expressed in the internationally accepted per mil (‰) standard notation relative to the Vienna Pee Dee belemnite. Isotopic results were calibrated against the NBS-19 international standard. Reproducibility for both  $\delta^{18}\text{O}$  and  $\delta^{13}\text{C}$  was better than 0.2‰, based upon multiple sample analyses. ICP-AES element (Ca, Mg, Sr, Fe, Mn) analyses were carried out on a Varian 725-ES spectrometer. During the preparation procedure, subsamples of 100–200 mg were dissolved in 4% nitric acid. Based upon

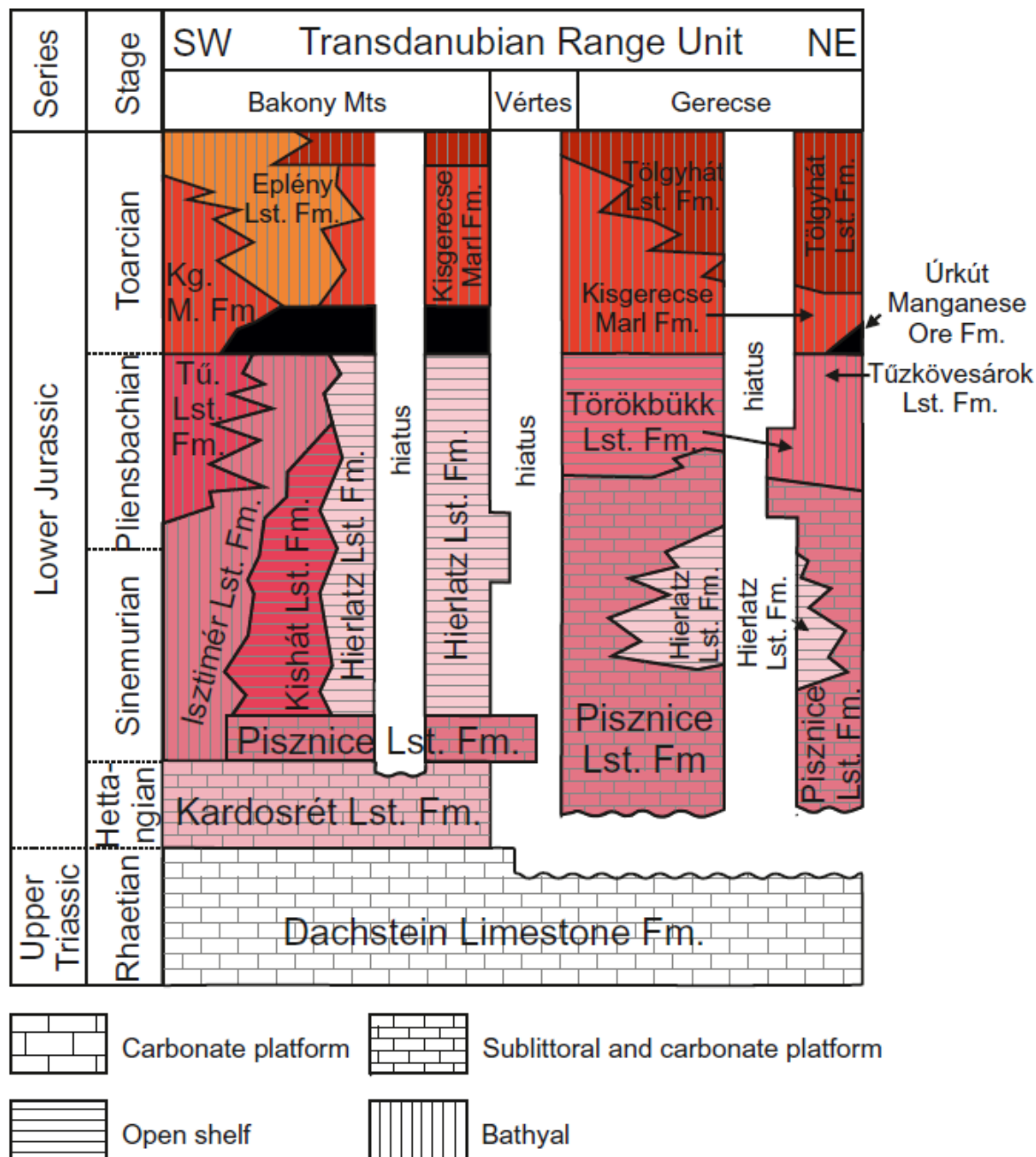


Fig. 3. Litho- and chronostratigraphic chart of the uppermost Triassic and Lower Jurassic formations in the Gerecse Hills and adjacent areas in the Transdanubian Range Unit, along a SW to NE transect. Colours approximate the appearance of these rocks in the field. The chart and inferred depositional environments are adapted from Fózy (2012) and Budai et al. (2018). Lst., Limestone.

analysis of duplicate samples, reproducibility was better than 4% of the measured concentration of each element. X-ray powder diffraction measurements were carried out in the laboratories of the Institute of Mineralogy and Geology at the University of Miskolc (Hungary) using a Bruker D8 Advance diffractometer, applying Cu-K $\alpha$  radiation, 40 mA tube current and 40 kV accelerating voltage, parallel beam geometry obtained with Göbel mirror in reflection geometry, Vantec-1 position-sensitive detector with 1° detector window opening and 0.007° 2 $\theta$ /14 s Bakony Mts Vértes Gerecse SW Transdanubian Range Unit NE Hills and adjacent areas in the Transdanubian Range Unit, along a SW to NE transect. Colours approximate the appearance of these rocks in the field. The chart and inferred depositional environments are adapted from Fózy (2012) and Budai et al. (2018). Lst., Limestone. goniometer speed. Identification of crystalline phases was done by the

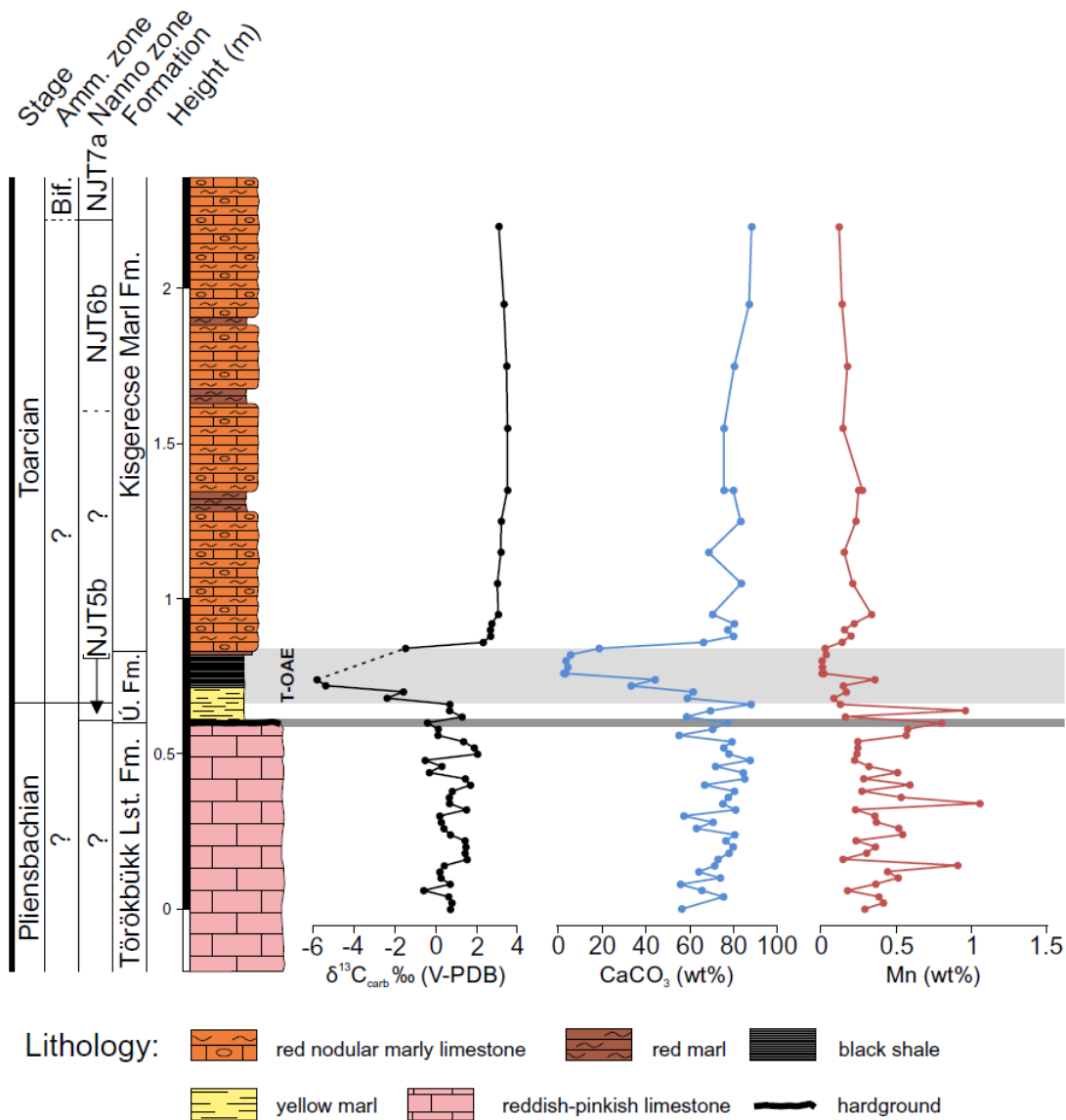
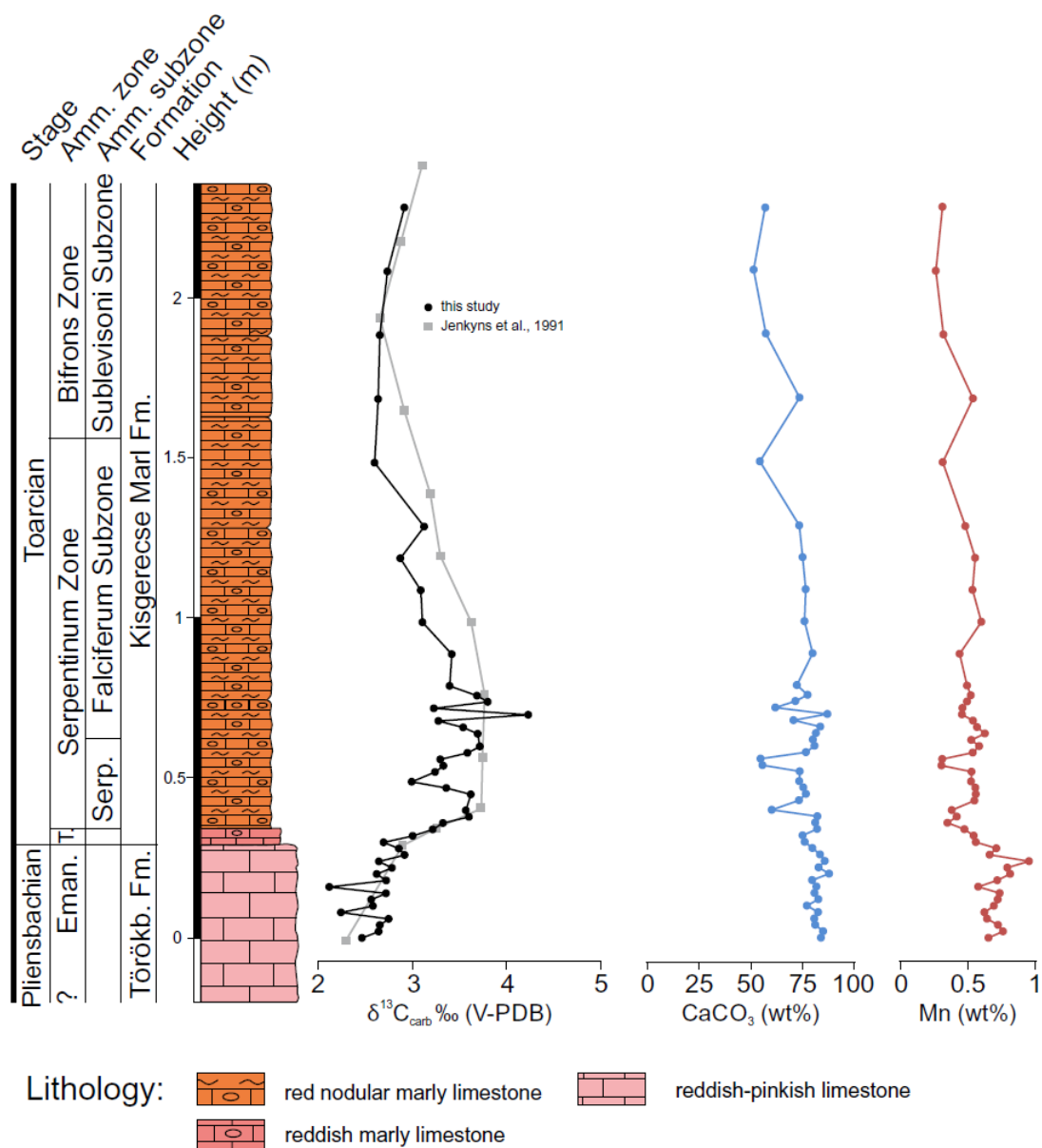


Fig. 4. Lithological log and geochemical data obtained from the Tölgyhát section. Ammonite biostratigraphy after Géczy (1984, 1985). Nannofossil biostratigraphy is from this study. Lst., Limestone; Bif., Bifrons Zone.

Search/Match algorithm (Marquart et al. 1979) in the Diffraction Plus EVA on the ICDD PDF2 (2005) database. Rietveld refinement (Bish and Post 1993) was performed using the TOPAS4 software with empirical instrument parameterization on the NIST SRM640d Si standard. Crystal structure data for calculations were obtained from the AMCSD [22] database. The 2  $\mu\text{m}$  grain size fraction was separated for oriented XRD measurements by gravitational separation in a distilled water column, where the settling time was determined using Stokes' Law. From every sample, two oriented specimens were prepared and both were measured in air-dry conditions. The first sample was measured after heating to 350 and 550°C, in order to observe structural collapse. The other sample was treated with ethylene glycol using the vapour method (Brunton 1955) to determine the swelling. Microscope slides for calcareous nannofossil analysis were made from 18 samples. A small amount of powdered rock was mixed with water before spreading onto a cover slide as homogeneously as possible (Bown and Young 1998). Cover slides were mounted onto microscope slides by Rhodopass were then studied using a Leica DM750P polarized microscope at 1000 $\times$  magnification. As the slides revealed a very poor nannofossil content, a minimum of three traverses per sample were analysed (c. 2 mm<sup>2</sup>). The preservation state of the nannofossils was estimated based on the degree of etching and overgrowth, according to Roth (1984). Calcareous nannofossil slides are curated at the Collections de Géologie de Lyon with an FSL number.





**Fig. 5.** Lithological log and geochemical data obtained from the Kisgerecse section. Ammonite biostratigraphy after Géczy (1984, 1985) and Kovács (2012). Grey curve: carbonate carbon isotope record from Jenkyns *et al.* (1991). Törökb. Fm., Törökbükk Limestone Fm.; Eman., Emaciatum Zone; T., Tenuicostatum Zone; Serp., Serpentinum Subzone.

## Results

**Calcareous nanofossil biostratigraphy** The nanofossil preservation is rather poor in the samples from the Tölgyhát section. Five samples are completely barren, and four others only contain *Schizosphaerella* spp., a taxon with uncertain affinities and no biostratigraphic value. Based on the presence of *Lotharingius crucicentralis* in the sample TH5, the NJT5b subzone of Ferreira *et al.* (2019) is identified at 0.65 m (Fig. 2; Table 2). The overlying interval spanning the Úrkút Fm. is barren, but from 1.2 m stratigraphically upwards calcareous nanofossils are present again. Significantly, the last occurrence of *Mitrolithus jansae* is recorded at 1.60 m. This disappearance event has been recently proposed by Ferreira *et al.* (2019) to define the base of the NJT6b subzone, which in several sections correlates with the aftermath of the Jenkyns Event. The following nanofossil event is the first occurrence of *Discorhabdus striatus*, which is considered as the marker of the NJ7, NJT7 and NJT7a zones (Bown and Cooper 1998; Mattioli and Erba 1999; Ferreira *et al.* 2019, respectively). This nanofossil zone correlates with the upper part of early Toarcian. Stable isotope and elemental geochemistry Bulk carbonate  $\delta^{13}\text{C}$  values from both the Tölgyhát and the Kisgerecse sections show a distinct pattern. At Tölgyhát, in the Törökbükk Fm., values are gently oscillating between  $-1$  and  $2$ ‰ (Figs 4 and 5). In the Úrkút Fm., in an interval not dated by nanofossils, a sharp negative CIE of c.  $6.5$ ‰ occurs

**Table 1.** Pearson correlation values (*r*) of  $\delta^{13}\text{C}$ ,  $\delta^{18}\text{O}$  and Sr/Ca ratios and their statistical significance (*p*) by sections and formations

	$\delta^{13}\text{C}$ and $\delta^{18}\text{O}$		$\delta^{13}\text{C}$ and Sr/Ca		$\delta^{18}\text{O}$ and Sr/Ca	
	Pearson ( <i>r</i> )	<i>p</i> -Value	Pearson ( <i>r</i> )	<i>p</i> -Value	Pearson ( <i>r</i> )	<i>p</i> -Value
<i>Kisgerecse</i>						
Törökbükk Limestone Fm.	0.03	0.39	−0.46	0.075	−0.32	0.18
Kisgerecse Marl Fm.	0.51	0.0038	−0.35	0.051	−0.05	0.38
<i>Tölgyhát</i>						
Törökbükk Limestone Fm.	0.60	0.00051	−0.25	0.147	−0.38	0.04
Úrkút Marl Fm.	0.87	0.0026	0.08	0.374	0.22	0.32
Kisgerecse Marl Fm.	−0.50	0.072	−0.62	0.022	0.47	0.09

within 10 cm, coincident with the change in lithology from the yellow marl to the black shale layer. The most negative value reaches  $-5.8\text{‰}$  (Fig. 4). Above this very negative value, within the black shale layer, five samples did not yield a sufficient amount of carbonate for analyses. The next  $\delta^{13}\text{C}$  value obtained immediately above the black shale near the base of the Kisgerecse Fm. captures the rebound phase of the negative CIE ( $-1.5\text{‰}$ ). Above the negative CIE in the Kisgerecse Fm. the  $\delta^{13}\text{C}$  curve remains nearly flat where values fall in a narrow range between 3 and  $3.5\text{‰}$  (Fig. 4). At Kisgerecse the  $\delta^{13}\text{C}$  record shows fluctuating values between 2.1 and  $2.9\text{‰}$  in the Pliensbachian part of the section (Fig. 5). Higher up, the  $\delta^{13}\text{C}$  curve indicates a positive excursion of c.  $1.5\text{‰}$  in the Tenuicostatum Zone and the lower half of the Serpentinum Subzone (Kovács 2012), reaching  $3.6\text{‰}$ . In the upper half of the Serpentinum Subzone and lower part of the Falciferum Subzone, values fluctuate between 3 and  $4.2\text{‰}$ , where the latter represents the most positive value (Fig. 5). Higher in the Falciferum Subzone the  $\delta^{13}\text{C}$  curve shows a slight negative trend up to the Bifrons Zone boundary, declining from 3.1 to  $2.6\text{‰}$ . In the Bifrons Zone the  $\delta^{13}\text{C}$  curve becomes nearly flat with values between 2.6 and  $2.9\text{‰}$  (Fig. 5). The  $\delta^{18}\text{O}$  data from the Tölgyhát section show large variability in the Törökbükk Fm. and the Úrkút Fm., where the values range between  $-10.4$  and  $-1.3\text{‰}$ . In the Kisgerecse Fm.  $\delta^{18}\text{O}$  values display less variability, within a range of  $1\text{‰}$ , between  $-2.1$  and  $-1.1\text{‰}$ . In the Kisgerecse section the  $\delta^{18}\text{O}$  record does not show any clear trend; the values fluctuate between  $-1.6$  and  $-2.6\text{‰}$ . Ca ICP-AES data from both the Tölgyhát and Kisgerecse sections were used to compute calcium carbonate content, considering carbonate minerals as the prevailing phase that contains Ca. The  $\text{CaCO}_3$  content varies between 55 and 88 wt% in the Törökbükk Fm. and subsequently drops sharply from 88 to 2.6 wt% in the Úrkút Fm., reaching the lowest values in the black shale layer (Fig. 4). Above the black shale,  $\text{CaCO}_3$  rises abruptly to c. 80 wt% and remains high, fluctuating between c. 70 and c. 83 wt% (Fig. 4). In the Kisgerecse section, there is a general decreasing trend in the  $\text{CaCO}_3$  curve, where values decline from c. 88 to c. 50 wt% (Fig. 5). The Sr/Ca ratio of samples from both the Tölgyhát and Kisgerecse sections is expressed in mmol/mol. Sr/Ca ratio values generally range between 0.13 and 0.44 mmol/mol in the Tölgyhát section with the exception of the black shale layer of the Úrkút Fm., where it increases suddenly to 1.85 mmol/mol and decreases to 0.24 mmol/mol at the top of the black shale layer (Fig. 6). Remarkably, the black shale layer also provided the lowest Ca (1.4 wt%) and Sr (34 ppm) concentrations. At the Kisgerecse section the Sr/Ca ratio does not show any clear pattern; values vary between 0.18 and 0.33 mmol/mol. Manganese concentration data obtained from ICP-AES analyses show very high variability within the Törökbükk Fm. in the Tölgyhát section where values are between 0.15 and 1 wt%. Surprisingly, Mn concentration in the Úrkút Fm. is the lowest within the entire section (0–0.3 wt%), reaching very low values (67 ppm) in the black shale layer (Fig. 4). The only level where exceptionally high [Mn] can be expected is the hardground layer at the base of the Úrkút Fm., which was excluded from sampling because samples were taken primarily for stable isotope analyses. Higher up in the Kisgerecse Fm. Mn concentration is less variable; it remains between 0.15 and 0.27 wt% (Fig. 4). The [Mn] in the Kisgerecse section is generally significantly lower than at Tölgyhát, showing higher values in the Törökbükk Fm. (0.06–0.1 wt%) and somewhat lower values in the Kisgerecse Fm. (0.03–0.06 wt%; Fig. 5).

#### Mineral composition

In the Tölgyhát section, calcite content is high in the Törökbükk Fm. (84–97 wt%), drops significantly to c. 50 wt% in the hardground layer that marks the base of the Úrkút Fm., and reaches the lowest values of 1–3 wt% in the yellow clay and the black shale. In the red marl at the base of the Kisgerecse Fm., calcite content increases to c. 50 wt% and reaches even higher values of 85–96 wt% upsection. In the higher part of

the Kisgerecse Fm. calcite content drops again to 62–66 wt% (Fig. 7). Detrital components such as quartz and clay minerals (illite, kaolinite and randomly interstratified illite/smectite) occur in very low concentrations in the Törökbükk Fm.: the proportion of quartz ranges from 1 to 5 wt% and that of illite is 2–7 wt%. Kaolinite is only present in the uppermost part of the formation, making up 2 wt%. In the Úrkút Fm., the abundance of both quartz and illite increases significantly to c. 30 and c. 33–41 wt%, respectively, whereas kaolinite remains subordinate at c. 0.5–1 wt% (Fig. 7). At the base of the Kisgerecse Fm., quartz and illite concentrations are high at c. 12 and c. 20 wt%, respectively, but they decrease higher up to 1–4 and 2–9 wt%. At the higher part of the Kisgerecse Fm. their proportion increases again to c. 10 and c. 20 wt% (Fig. 7). Other detrital components make a negligible contribution to the total mineral composition. Randomly interstratified illite/smectite and microcline make up 2–11 and 4–11 wt% of the Úrkút Fm., but they reappear in the higher part of the Kisgerecse Fm. at only 1–3 wt%. Muscovite is only present in the black shale layer of the Úrkút Fm. (c. 9 wt%). The hardground layer at the base of the Úrkút Fm. is distinguished by its very high proportion of pyrolusite (51 wt%). Full details of the geochemical and mineralogical data are provided as Supplementary Material in Table S1.

## Discussion

### *Effect of diagenesis*

Screening for potential diagenetic overprint is important before the evaluation and a comprehensive palaeoenvironmental and palaeoclimatic interpretation of stable isotope data. An assessment of the relationship between carbon and oxygen isotopes in marine carbonates is often applied in order to evaluate the degree of diagenetic alteration (Brand and Veizer 1981). Generally, a positive correlation between the two isotopic ratios is considered as a sign of the influence of meteoric water during diagenesis. However, such correlation might not represent a secondary diagenetic effect if there is no sign of subaerial exposure of sediments or the changes in  $\delta^{13}\text{C}$  and  $\delta^{18}\text{O}$  both record major environmental perturbations and climate change that are reflected in isotopic changes, such as the case during the Jenkyns Event (Hermoso et al. 2012; Ullmann et al. 2014; Schobben et al. 2016). Additionally, lithological changes in marine carbonate successions may display differential diagenetic alteration in  $\delta^{13}\text{C}$  and  $\delta^{18}\text{O}$  (Rosales et al. 2001). Therefore, we tested the correlation between carbon and oxygen isotopes, considering also the distinct lithologies of the studied sections (Table 1). At the Kisgerecse section,  $\delta^{13}\text{C}$  and  $\delta^{18}\text{O}$  values indicate no significant correlation in the Törökbükk Fm. (Pearson  $r = 0.03$ ) and in the Kisgerecse Fm. (Pearson  $r = 0.51$ ; Table 1) and the values fall in the field of normal marine limestones (Knauth and Kennedy 2009; Fig. 6), which suggests good preservation of the primary isotopic signal in this section. In the Tölgyhát section  $\delta^{13}\text{C}$  and  $\delta^{18}\text{O}$  data show a higher correlation in the Törökbükk Fm. (Pearson  $r = 0.6$ ; Table 1) and also a larger variation in  $\delta^{18}\text{O}$  and a much lower one in  $\delta^{13}\text{C}$  (Fig. 6), suggesting a secondary diagenetic effect and a water–rock interaction with a limited amount of meteoric water, which generally has little impact on  $\delta^{13}\text{C}$  (Lohmann 1988). The diagenetic effect on the Úrkút Fm. appears more significant on the basis of  $\delta^{13}\text{C}$ – $\delta^{18}\text{O}$  correlation (Pearson  $r = 0.87$ ; Table 1). Environmental changes related to the Jenkyns Event could lead to this strong correlation in the Úrkút Manganese Ore; however, such negative  $\delta^{18}\text{O}$  data (greater than  $-7\text{‰}$ ) suggests that the oxygen isotope composition was probably affected by later diagenetic overprint to some degree. Additionally, the most negative  $\delta^{13}\text{C}$  values (c.  $-5$ – $-6\text{‰}$ ) are lower than in published early Toarcian bulk carbonate records (Hesselbo et al. 2007; Hermoso et al. 2009; Bodin et al. 2016). Such low values are commonly related to organic matter remineralization and precipitation of  $^{13}\text{C}$ -depleted carbonate in organic-rich mudstones, forming during early diagenesis under anaerobic conditions when sulfate reduction takes place (Bodin et al. 2016; Wohlwend et al. 2016; Arabas et al. 2017). Although this possibility cannot be excluded, the stratigraphic position (Fig. 3) and the facies characteristics suggest that the negative CIE in the Úrkút Manganese Ore Fm. at Tölgyhát represents the Jenkyns Event. Regional correlation provides further support as this formation is much thicker and particularly manganese-rich in the Bakony Mts., where it yielded organic carbon isotope values between  $-32$  and  $-34\text{‰}$  that are typical for the negative CIE (Polgári et al. 2016). In the higher part of the section, in the Kisgerecse Fm., a negative correlation between  $\delta^{13}\text{C}$  and  $\delta^{18}\text{O}$  (Pearson  $r = -0.5$ ) and a normal marine range of values (Fig. 6) suggest good preservation of the isotopic signal.

Calcareous nannofossils of the Tölgyhát section, where present, are poorly preserved with traces of overgrowth (Table 2). This suggests some secondary diagenetic precipitation of calcite during burial (Adelsoeck et al. 1973). Trace elements in carbonate, primarily Mn and Sr, and their ratios to Ca are also widely used as tools for screening diagenetic alteration in carbonate sediments. The Mn concentration increases whereas Sr decreases during dissolution and recrystallization of carbonates owing to interaction with meteoric water

(Brand et al. 2012a; 2012b; Schobben et al. 2016). In this case,

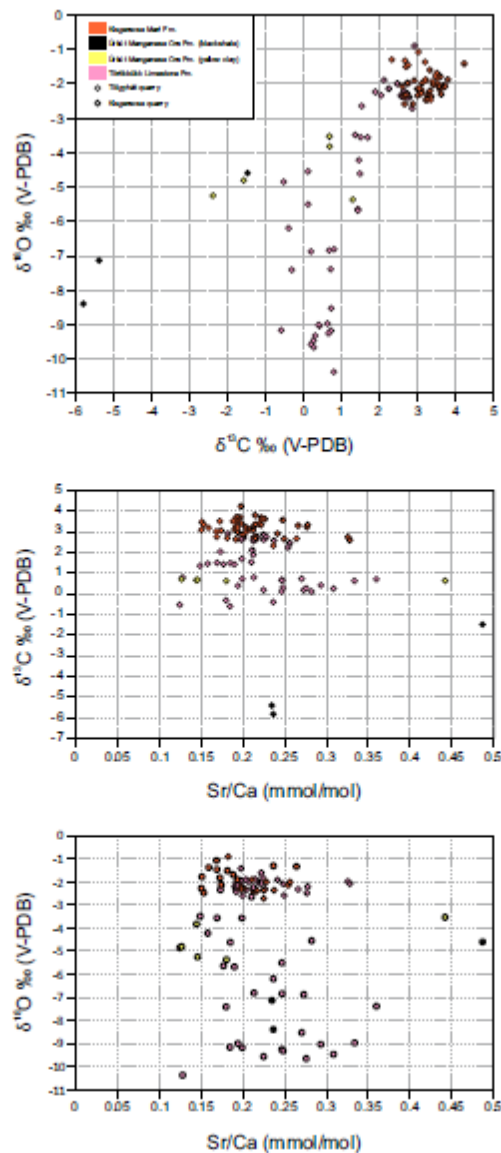


Fig. 6. Scatter plots of carbon and oxygen isotope and Sr/Ca ratios from the Tölgyhát and Kisgeregse sections for diagenetic screening.

however, Mn is not a reliable elemental indicator to use since the studied pelagic formations are particularly rich in Mn oxides (Figs 4 and 5) and it is generally present as dispersed microscopic to macroscopic nodules and coating on bio- and intraclasts, which could not be avoided during sampling. The Sr content, on the other hand, is not biased; therefore, the Sr/Ca ratio was additionally used for screening the diagenetic overprint (Fig. 6). Neither  $\delta^{13}\text{C}$  nor  $\delta^{18}\text{O}$  shows a significant positive correlation with Sr/Ca in any of the samples from both sections and the different formations, which further supports the good preservation of the isotopic signals. In summary, the carbon isotope records from the Kisgeregse and Tölgyhát sections indicate good preservation of original environmental signals, whereas the oxygen isotope record is potentially altered by diagenesis to a certain degree; therefore it is not suitable for palaeoclimatic interpretation. However, the  $\delta^{13}\text{C}$  data from the Úrkút Manganese Ore Fm. might have been affected by organic matter remineralization to some extent.

#### *Carbon isotope records and integrated stratigraphic correlation*

Previously, Jenkyns and Clayton (1986) and Jenkyns et al. (1991) reported carbon isotope and stratigraphic information from two localities of the Gerecse Hills (Kisgeregse and Bányahegy) and investigated their relationship with other Tethyan localities. Here, we constructed high-resolution geochemical records and

nannofossil biostratigraphy for the Tölgyhát and Kisgerecs sections in order to further explore the impact of the Jenkyns Event in the pelagic realm. A correlation between the two studied sections from the Gerecs Hills

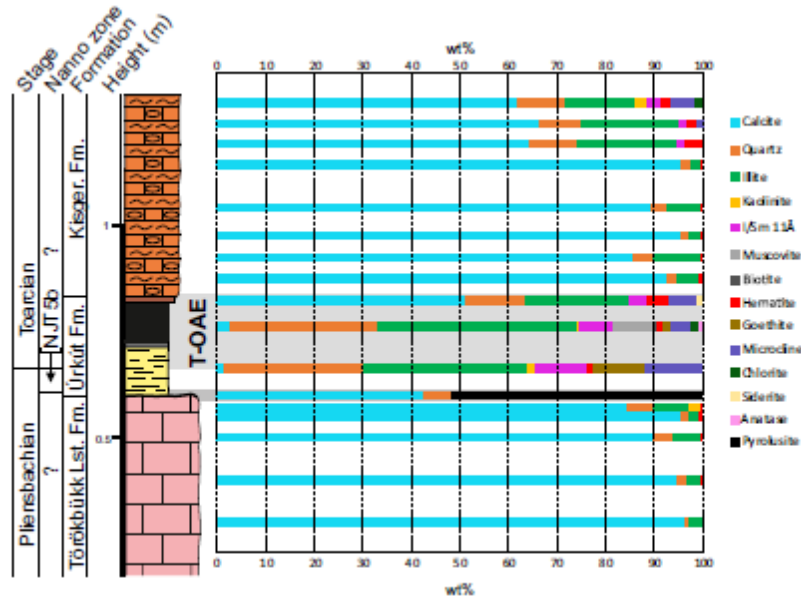


Fig. 7. Mineral composition of sampled layers in the Tölgyhát section.

with the stratigraphically continuous and complete sedimentary record of the Peniche section from the Lusitanian Basin (Portugal; Hesselbo et al. 2007; Rocha et al. 2016) has been carried out using the combination of biostratigraphical and high-resolution carbon isotope data (Fig. 8). The comprehensively studied Peniche section serves as the global boundary stratotype section and point for the Toarcian Stage (Rocha et al. 2016), and as such, correlates with all other sections worldwide that record the Jenkyns Event. The Pliensbachian part of the Törökbükk Limestone of the Tölgyhát and Kisgerecs sections does not show any significant  $\delta^{13}\text{C}$  trends. Its latest Pliensbachian age (Jenkyns et al. 1991; Császár et al. 1998) is also confirmed in the Tölgyhát section by the presence of the NJT5b nannofossil zone that spans the Pliensbachian/Toarcian boundary (Ferreira et al. 2019). Together with  $\delta^{13}\text{C}$  data, this suggests that the deposition of this facies ended in the latest Pliensbachian before the Pliensbachian/Toarcian Event (Littler et al. 2010; Ait-Ito et al. 2017). The Pliensbachian carbon isotope data from Tölgyhát varies within a similar range compared with Peniche (between c. 0 and 1‰), whereas at Kisgerecs the values are slightly higher, between 2 and 3‰ (Fig. 8). Considering the biostratigraphical uncertainties and the proximity to Tölgyhát, this probably suggests that the  $\delta^{13}\text{C}$  record at Kisgerecs does not include the uppermost Pliensbachian. Such positive values were reported from the Margaritatus Zone (Suan et al. 2010; Silva et al. 2011); however, the absence of precise biostratigraphic constraints precludes an unambiguous correlation. The Pliensbachian/Toarcian Event is probably associated with the onset of greenhouse gas release from the Karoo–Ferrar LIP and it is characterized by a distinct negative CIE in the lowest part of the Polymorphum Zone or its equivalent, the Tenuicostatum Zone (Hesselbo et al. 2007; Littler et al. 2010; Ait-Ito et al. 2017) and the NJT5c nannofossil zone (Ferreira et al. 2019). This negative CIE is well represented at Peniche (Hesselbo et al. 2007), but it is stratigraphically not documented in the Gerecs sections. The Pliensbachian/Toarcian Event is followed by a broad positive  $\delta^{13}\text{C}$  excursion, probably related to enhanced organic production and carbon burial on a global scale in the Polymorphum (= Tenuicostatum) Zone preceding the pronounced negative CIE at the T-OAE (Hesselbo et al. 2007; Hermoso et al. 2012; Müller et al. 2020b). This positive excursion is also missing at both the Tölgyhát and Kisgerecs sections, only a highly condensed c. 5 cm thick bed is assigned to the Tenuicostatum Zone (Géczy 1984; 1985; Kovács 2012; Fig. 8). According to the astrochronological record reported by Suan et al. (2008b) and confirmed by Huang and Hesselbo (2014) for the Peniche section, a record of a c. 800 kyr interval with the Pliensbachian/Toarcian Event and the subsequent positive excursion is missing from Tölgyhát, but is at least partly present in Kisgerecs in the highly condensed Tenuicostatum Zone bed (Fig. 8). The hallmark of the Jenkyns Event is a sharp negative CIE of c. 4–6‰ that commonly falls into the uppermost Tenuicostatum and the lower Serpentinum ( $\approx$  Levisoni) Zones, that is globally recognized and is present in biogenic calcite, micrite and organic matter as well (Hesselbo et al. 2000; van Breugel et al. 2006; Hesselbo



et al. 2007; Hermoso et al. 2009; Suan et al. 2010; Caruthers et al. 2011; Gröcke et al. 2011; Izumi et al. 2012; Al-Suwaidi et al. 2016; Bodin et al. 2016). This CIE is a useful tool for stratigraphic

**Table 2.** Distribution of nanofossil taxa in the Tölgyhát section

Label	Sample	Height (cm)	<i>Schizosphaerella</i>	<i>Micrathus javae</i>	<i>Micrathus elegans</i>	<i>Crepidulus erasus</i>	<i>Tubirhabdus parvus</i>	<i>Similiscutum fuchii</i>	<i>large Similiscutum fuchii</i>	<i>Similiscutum novum</i>	<i>Loxaringia crucicentris</i>	<i>Loxaringia frodoii</i>	<i>Loxaringia hauffii</i>	<i>Loxaringia sigillata</i>	<i>Loxaringia umbonensis</i>	<i>Discorhabdus ignotus</i>	<i>Discorhabdus aratus</i>	<i>Large Calymene</i>	Unidentified coecolith	Preservation	Nanofossil zone	Age
TH	210	270	.	.	.	.	.	.	.	.	.	.	.	.	.	.	.	.	.	VVP	NJT7a	Early-middle Toarcian
TH	166	226	.	.	.	.	.	.	.	.	.	.	.	.	.	.	.	.	.	B		
TH	163	223	.	.	.	.	.	.	.	.	.	.	.	.	.	.	.	.	.	VVP		
TH	151	211	.	.	.	.	.	.	.	.	.	.	.	.	.	.	.	.	.	VVP	NJT6b	Early Toarcian
TH	120	180	.	.	.	.	.	.	.	.	.	.	.	.	.	.	.	.	.	B		
TH	100	160	.	.	.	.	.	.	.	.	.	.	.	.	.	.	.	.	.	VVP	?	
TH	73	133	.	.	.	.	.	.	.	.	.	.	.	.	.	.	.	.	.	VVP		
TH	60	120	.	.	.	.	.	.	.	.	.	.	.	.	.	.	.	.	.	VVP		
TH	33	93	.	.	.	.	.	.	.	.	.	.	.	.	.	.	.	.	.	B		
TH	19	79	.	.	.	.	.	.	.	.	.	.	.	.	.	.	.	.	.	B		
TH	12G	72	.	.	.	.	.	.	.	.	.	.	.	.	.	.	.	.	.	VVP		
TH	9	69	.	.	.	.	.	.	.	.	.	.	.	.	.	.	.	.	.	BB		
TH	8	68	.	.	.	.	.	.	.	.	.	.	.	.	.	.	.	.	.	nB		
TH	5	65	.	.	.	.	.	.	.	.	.	.	.	.	.	.	.	.	.	VVP	NJT5b	
TH	0	60	.	.	.	.	.	.	.	.	.	.	.	.	.	.	.	.	.	nB	?	Late Pliensbachian
TH	-30	30	.	.	.	.	.	.	.	.	.	.	.	.	.	.	.	.	.	nB		
TH	-60	0	.	.	.	.	.	.	.	.	.	.	.	.	.	.	.	.	.	VVP		

Nanofossil data: ., present; ., absent; \*, last occurrence; \*, first occurrence; -, single occurrence of biostratigraphic significance.

correlation of different sections. The T-OAE and negative CIE (associated with the Jenkyns Event) are well represented at Peniche with a duration of c. 600–650 kyr (Suan et al. 2008b; Huang and Hesselbo 2014) but they are only recorded in the Tölgyhát section in the Gerecse Hills, in the upper half of the Úrkút Fm. in a highly condensed c. 24 cm interval covering the upper half of the yellow marl and the black shale layer (Fig. 8). The negative CIE is followed by another positive excursion (a rebound), with an approximate duration of c. 480 kyr as determined in Peniche and at other localities (Huang and Hesselbo 2014) where the sedimentation rate was fairly constant, and the record continues in the upper Levisoni Zone (Hesselbo et al. 2007; Suan et al. 2015; Xu et al. 2018; Ruebsam and Al-Husseini 2020) or upper NJT6a zone (Ferreira et al. 2019). This interval is at least partly recognized at both Tölgyhát and Kisgeresce (Fig. 8).

#### Impact of environmental change on pelagic carbonate systems

Multiple studies have suggested a calcification crisis that spans the Jenkyns Event (Mattioli et al. 2009; Trecalli et al. 2012; Ettinger et al. 2021), although brachiopod shell-based  $\delta^{11}\text{B}$ -pH data and a carbonate saturation model imply that the development of triggering factors commenced earlier, with the Pliensbachian/Toarcian Event (Krencker et al. 2020; Müller et al. 2020a). Shallow-water carbonate platforms, carbonate production in epicontinental basins and hemipelagic–pelagic settings open to the Tethys Ocean were all severely affected (Mattioli et al. 2009; Trecalli et al. 2012; Suan et al. 2018; Müller et al. 2020b). Several mechanisms have been postulated for interpreting this calcification crisis. First, increasing global seawater temperature and associated acceleration of hydrological cycle and eutrophication of the water column (Suan et al. 2008a), or alternatively, thermohaline stratification of surface waters, triggered a decrease in nutrient levels of surface waters, adversely affecting the calcareous phytoplankton (Mattioli et al. 2009). Second, a eustatic sea-level rise may have resulted in the drowning of carbonate platforms and, as a consequence, also in carbonate shortage in epicontinental basinal settings (Bodin et al. 2010; Léonide et al. 2012; Pittet et al. 2014), which could also explain the carbonate shortage in hemipelagic–pelagic ocean-facing basins (Müller et al. 2020b). Third, ocean acidification could have developed owing to the input of excess  $\text{CO}_2$  into the ocean–atmosphere system, lowering both the seawater pH and calcite saturation level ( $\Omega_c$ ; Trecalli et al. 2012; Müller et al. 2020a; Ettinger et al. 2021). Fourth, enhanced continental weathering and an increase in siliciclastic supply may have led to carbonate factory shutdown in shallow-water carbonate platforms (Krencker et al. 2020).

The results of chemostratigraphic correlation in combination with biostratigraphy of the continuous and complete Peniche section with Tölgyhát and Kisgeresce (Fig. 8) indicate significant condensation and hiatuses at certain levels of these pelagic carbonate successions in the western Tethys. The temporal

coincidence of these sedimentary features with the Pliensbachian/Toarcian Event and the Jenkyns Event suggests that global warming and concomitant calcification crises substantially affected the pelagic carbonate systems in the Gerecse. A major hiatus in these lower Toarcian sections occurs in the *Tenuicostatum*

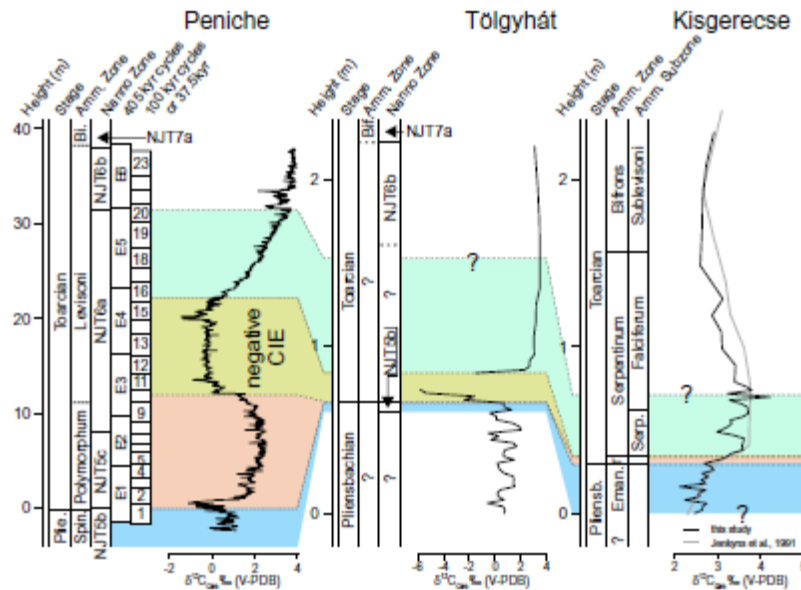


Fig. 8. Chemostratigraphic correlation of the Tölgyhát and Kisgercse sections with the continuous reference record of the Toarcian global boundary stratotype section and point section at Peniche, Portugal.  $\delta^{13}\text{C}$  curve and stratigraphic scale for Peniche are from Hesselbo *et al.* (2007). Nannofossil biostratigraphy of Peniche are from Ferrel *et al.* (2019). Astrochronology is from Huang and Hesselbo (2014). Ammonite biostratigraphy for the Tölgyhát section is from Géczy (1984). Calcareous nannofossils are from this study. Ammonite biostratigraphy of the Kisgercse section is from Géczy (1984, 1985) and Kovács (2012). Grey curve: bulk carbon isotope data by Jenkyns *et al.* (1991).

Zone, which is commonly associated with hardgrounds on the top of the upper Pliensbachian-Törökbükk Fm. (Császár *et al.* 1998; Kovács 2012). The absence of the *Tenuicostatum* Zone, with the exception of the Kisgercse section, and the sudden drop of  $\text{CaCO}_3$  from c. 80 to 3 wt% simultaneously with the negative CIE in the Tölgyhát section, suggest that adverse environmental conditions leading to the shutdown of pelagic carbonate production developed in the Gerecse basin around the Pliensbachian/Toarcian Event and persisted during the Jenkyns Event. Elsewhere, brachiopod boron isotope-based pH reconstruction, carbonate saturation state models and sedimentological evidence from shallow marine carbonate platforms previously supported that low pH conditions indeed started to develop at the Pliensbachian/Toarcian Event and seawater pH fluctuated, reaching its minimum immediately prior to and during the Jenkyns Event (Müller *et al.* 2020a; Ettinger *et al.* 2021). Hardgrounds and gaps are often associated with the Pliensbachian/Toarcian boundary and the lower Toarcian at other Tethyan localities as well (e.g. Léonide *et al.* 2012; Pittet *et al.* 2014; Arabas *et al.* 2017; Fantasia *et al.* 2018; Rosales *et al.* 2018). The appearance of hardgrounds at the same stratigraphic level in the Adriatic Carbonate Platform has been explained by submarine dissolution owing to shoaling of carbonate compensation depth as a consequence of  $\text{CO}_2$ -rich, undersaturated bottom waters as a result of massive  $\text{CO}_2$  input into the ocean-atmosphere system from the Karoo-Ferrar LIP (Ettinger *et al.* 2021). This scenario could potentially also be applicable for pelagic carbonate successions such as those at Tölgyhát and Kisgercse. Additionally, the marine transgression associated with the Jenkyns Event (Haq 2018; Ruebsam *et al.* 2019) probably played a role in the drowning of nearby platforms (Léonide *et al.* 2012), thereby reducing carbonate sediment supply into the basins and also moving the source of detrital input further away. Taken together, these factors arrested the carbonate sedimentation and resulted in a condensed record of the Jenkyns Event and contemporaneous gaps in the pelagic successions of the Gerecse basin. Mineralogical composition of detrital components of the Tölgyhát section indicates high illite and quartz content for the Úrkút Fm., but negligible kaolinite, randomly interstratified illite/smectite and microcline (Fig. 7). Kaolinite is often present in abundance in NW European sections where it has been considered as an indicator for intense continental weathering with high water-rock ratio, owing to the global warming and accelerated hydrological cycle during the Jenkyns Event (Raucsik and Varga 2008; Dera *et al.* 2009). The low kaolinite content in the Úrkút Fm. at Tölgyhát suggests a very distal position of the Gerecse basin, similar to the observations from the Lombardian Basin (Fantasia *et al.* 2018).

## Conclusions

In this study, we present new high-resolution geochemical data from two upper Pliensbachian – lower Toarcian pelagic sections from the Gerecse Hills (Hungary), Tölgyhát and Kisgerecse, complemented by new nannofossil biostratigraphic data from Tölgyhát. The deposition of the pelagic successions that consist of limestone, marl and black shale in these sections took place in proximity to the open Tethys Ocean near its northwestern shelf. The carbon isotope record of the Tölgyhát section shows that the negative CIE related to the Jenkyns Event is only present in a 24 cm thick highly condensed black shale layer, where bulk calcium carbonate and calcite content drop significantly from c. 80 to 3 wt%. In the Kisgerecse section, this isotope anomaly is not recorded due to a stratigraphic gap. The stratigraphic position of gaps, condensation and hardgrounds in these successions coincides with the Pliensbachian/Toarcian Event and the Jenkyns Event, suggesting that the pelagic carbonate system was severely affected by calcification crises, probably owing to large-scale CO<sub>2</sub> emission coincident with these events. Additionally, a sea-level rise during the Jenkyns Event could significantly decrease carbonate and siliclastic material input, facilitating sedimentary condensation and the development of hiatuses. Our results add to a growing body of evidence that perturbations of the Jenkyns Event were global in extent and severely affected different sedimentary environments, including pelagic carbonate depositional systems.

**Acknowledgements** Help in sampling in the field was provided by Mariann Bosnakoff, Dóra Kesjár and Zoltán Szentesi. László Fodor, Orsolya Sztanó and students of Eötvös Loránd University's geology field school are thanked for their inspiration and discussions about the geology of Gerecse Hills. Constructive reviews of Stéphane Bodin and Andrew Caruthers and additional suggestions of editor Luís Vitor Duarte helped to improve the manuscript significantly. This study received funding by the National Research, Development and Innovation Office of Hungary (grants OTKA NN 128702 and K 135309). The research was also supported by the European Union and the State of Hungary, co-financed by the European Regional Development Fund in the project of GINOP-2.3.2.-15- 2016- 00009 'ICER'. This is a contribution to IGCP Project 655 and MTA-MTM-ELTE Paleo contribution no. 345. Author contributions TM: formal analysis (equal), investigation (lead), writing – original draft (lead), writing – review & editing (lead); GDP: conceptualization (supporting), formal analysis (equal), investigation (supporting), writing – original draft (supporting), writing – review & editing (supporting); EM: formal analysis (supporting), investigation (supporting), writing – original draft (supporting); MZL: formal analysis (supporting), investigation (supporting), writing – original draft (supporting); FK: formal analysis (supporting), investigation (supporting); JP: conceptualization (lead), funding acquisition (lead), supervision (lead), writing – original draft (supporting), writing – review & editing (supporting). Funding This work was supported by grants from the Hungarian Scientific Research Fund (NN128702 and K135309) to József Pálfi and from the Nemzeti Kutatási Fejlesztési és Innovációs Hivatal (GINOP-2.3.2.-15-2016- 00009 'ICER') to Tamás Müller.

**Data availability** All data generated or analysed during this study are included in this published article (and its supplementary information files).

## References

- Adelseck, C.G., Geehan, G.W. and Roth, P.H. 1973. Experimentalevidence for the selective dissolution and overgrowth of calcareous nannofossils during diagenesis. *Geological Society of America Bulletin*, 84, 2755–2762.
- Ait-Ito, F.Z., Price, G.D., Addi, A.A., Chafiki, D. and Mannani, I. 2017. Bulk-carbonate and belemnite carbon-isotope records across the Pliensbachian–Toarcian boundary on the northern margin of Gondwana (Issouka, Middle Atlas, Morocco). *Palaeogeography, Palaeoclimatology, Palaeoecology*, 466, 128–136
- Al-Suwaidi, A.H., Hesselbo, S.P. et al. 2016. The Toarcian Oceanic Anoxic Event (Early Jurassic) in the Neuquén Basin, Argentina: a reassessment of age and carbon isotope stratigraphy. *The Journal of Geology*, 124, 171–193, <https://doi.org/10.1086/684831>
- Arabas, A., Schlögl, J. and Meister, C. 2017. Early Jurassic carbon and oxygen isotope records and seawater temperature variations: insights from marine carbonate and belemnite rostra (Pieniny Klippen Belt, Carpathians). *Palaeogeography, Palaeoclimatology, Palaeoecology*, 485, 119–135, <https://doi.org/10.1016/j.palaeo.2017.06.007>
- Bailey, T.R., Rosenthal, Y., McArthur, J.M., van de Schootbrugge, B. and Thirlwall, M.F. 2003. Paleooceanographic changes of the Late Pliensbachian–Early Toarcian interval: a possible link to the genesis of an Oceanic Anoxic Event. *Earth and Planetary Science Letters*, 212, 307–320, [https://doi.org/10.1016/S0012-821X\(03\)00278-4](https://doi.org/10.1016/S0012-821X(03)00278-4)
- Bish, D.L. and Post, J.E., 1993. Quantitative mineralogical analysis using the Rietveld full-pattern fitting method. *American Mineralogist*, 78, 932–940.
- Bodin, S., Mattioli, E., Fröhlich, S., Marshall, J.D., Boutib, L., Lahsini, S. and Redfern, J. 2010. Toarcian carbon isotope shifts and nutrient changes from the Northern margin of Gondwana (High Atlas, Morocco, Jurassic): palaeoenvironmental implications. *Palaeogeography, Palaeoclimatology, Palaeoecology*, 297, 377–390, <https://doi.org/10.1016/j.palaeo.2010.08.018>

Bodin, S., Krencker, F.N., Kothe, T., Hoffmann, R., Mattioli, E., Heimhofer, U. and Kabiri, L. 2016. Perturbation of the carbon cycle during the late Pliensbachian–early Toarcian: new insight from high-resolution carbon isotope records in Morocco. *Journal of African Earth Sciences*, 116, 89–104, <http://doi.org/10.1016/j.jafrearsci.2015.12.018>

Bown, P.R. and Cooper, M.K.E. 1998. Calcareous nannofossils biostratigraphy. In: Bown, P.R. (ed.) *Calcareous Nannoplankton Biostratigraphy*. British Micropaleontological Press, 34–85.

Bown, P.R. and Young, J.R. 1998. Techniques. In: Bown, P.R. (ed.) *Calcareous Nannoplankton Biostratigraphy*. British Micropaleontological Press, 16–28.

Brand, U. and Veizer, J. 1981. Chemical diagenesis of a multicomponent carbonate system; 2, Stable isotopes. *Journal of Sedimentary Research*, 51, 987–997, <https://doi.org/10.1306/212f7df6-2b24-11d7-8648000102c1865d>

Brand, U., Jiang, G., Azmy, K., Bishop, J. and Montanez, I.P. 2012a. Diagenetic evaluation of a Pennsylvanian carbonate succession (Bird Spring Formation, Arrow Canyon, Nevada, USA)-1: Brachiopod and whole rock comparison. *Chemical Geology*, 308, 26–39, <https://doi.org/10.1016/j.chemgeo.2012.03.017>

Brand, U., Posenato, R., Came, R., Affek, H., Angiolini, L., Azmy, K. and Farabegoli, E. 2012b. The end-Permian mass extinction: a rapid volcanic CO<sub>2</sub> and CH<sub>4</sub>-climatic catastrophe. *Chemical Geology*, 322, 121–144, <https://doi.org/10.1016/j.chemgeo.2012.06.015>

Brunton, G. 1955. Vapour pressure glycolation of oriented clay minerals. *American Mineralogist*, 40, 124–126.

Bucefalo Palliani, R., Mattioli, E. and Riding, J. 2002. The response of marine phytoplankton and sedimentary organic matter to the early Toarcian (Lower Jurassic) oceanic anoxic event in northern England. *Marine Micropaleontology*, 46, 223–245, [https://doi.org/10.1016/S0377-8398\(02\)00064-6](https://doi.org/10.1016/S0377-8398(02)00064-6)

Budai, T., Fodor, L. et al. 2018. A Gerecse hegység földtana. Magyarázó a Gerecse hegység földtani térképéhez (1:50 000). (Geology of the Gerecse Mountains. Explanatory book to the geological map of the Gerecse Mountains (1:50 000)), Budapest, Magyar Bányászati és Földtani Szolgálat (Hungarian Mining and Geological Survey), Magyarország tájegységi térképsorozata (Regional map series of Hungary).

Caruthers, A.H., Gröcke, D.R. and Smith, P.L. 2011. The significance of an Early Jurassic (Toarcian) carbon isotope excursion in Haida Gwaii (Queen Charlotte Islands), British Columbia, Canada. *Earth and Planetary Science Letters*, 307, 19–26, <https://doi.org/10.1016/j.epsl.2011.04.013>

Caruthers, A.H., Smith, P.L. and Gröcke, D.R. 2014. The Pliensbachian–Toarcian (Early Jurassic) extinction: a North American perspective. *Geological Society of America Special Papers*, 505, 225–243 [https://doi.org/10.1130/2014.2505\(11\)](https://doi.org/10.1130/2014.2505(11))

Caswell, B.A., Coe, A.L. and Cohen, A.S. 2009. New range data for marine invertebrate species across the early Toarcian (Early Jurassic) mass extinction. *Journal of the Geological Society*, 166, 859–872, <https://doi.org/10.1144/0016-76492008-0831>

Cohen, A.S., Coe, A.L., Harding, S.M. and Schwark, L. 2004. Osmium isotope evidence for the regulation of atmospheric CO<sub>2</sub> by continental weathering. *Geology*, 32, 157–160, <https://doi.org/10.1130/g20158.1>

Császár, G., Galács, A. and Vörös, A. 1998. A gerecsei jura – fácieskérdések, alpi analógiák. [Jurassic of the Gerecse Mountains, Hungary: facies and Alpine analogies]. *Földtani Közlöny*, 128, 397–435.

Danise, S., Twitchett, R.J., Little, C.T. and Clémence, M.E. 2013. The impact of global warming and anoxia on marine benthic community dynamics: an example from the Toarcian (Early Jurassic). *PLoS One*, 8, e56255, <https://doi.org/10.1371/journal.pone.0056255>

Dera, G., Pellenard, P., Neige, P., Deconinck, J.F., Pucéat, E. and Dommergues, J.L. 2009. Distribution of clay minerals in Early Jurassic Peritethyan seas: palaeoclimatic significance inferred from multiproxy comparisons. *Palaeogeography, Palaeoclimatology, Palaeoecology*, 271, 39–51, <https://doi.org/10.1016/j.palaeo.2008.09.010>

Dulai, A. 1998. Early Jurassic brachiopods from the basal layers of the Pisznice Limestone of Lábatlan (Gerecse Mts, Hungary). *Annales historico-naturales Musei nationalis hungarici*, 90, 35–55.

Ettinger, N.P., Larson, T.E., Kerans, C., Thibodeau, A.M., Hattori, K.E., Kacur, S.M. and Martindale, R.C. 2021. Ocean acidification and photic-zone anoxia at the Toarcian Oceanic Anoxic Event: insights from the Adriatic Carbonate Platform. *Sedimentology*, 68, 63–107, <https://doi.org/10.1111/sed.12786>

Fantasia, A., Föllmi, K.B., Adatte, T., Spangenberg, J.E. and Montero-Serrano, J.C. 2018. The Early Toarcian oceanic anoxic event: Paleoenvironmental and paleoclimatic change across the Alpine Tethys (Switzerland). *Global and Planetary Change*, 162, 53–68, <https://doi.org/10.1016/j.gloplacha.2018.01.008>

Ferreira, J., Mattioli, E. et al. 2019. Western Tethys Early and Middle Jurassic calcareous nannofossil biostratigraphy. *Earth-Science Reviews*, 197, 102908, <https://doi.org/10.1016/j.earscirev.2019.102908>

Fozy, I. (ed.) 2012. Magyarország litosztratiográfiai alapegységei. Jura [Lithostratigraphic Units of Hungary. Jurassic]. Hungarian Geological Society, Budapest. Fülöp, J. 1976. The Mesozoic basement horst blocks of Tata. *Geologica Hungarica, series Geologica*, 16, 1–228.

Galács, A., Császár, G., Géczy, B. and Kovács, Z. 2010. Ammonite stratigraphy of a Toarcian (Lower Jurassic) section on Nagy-Pisznice Hill (Gerecse Mts, Hungary). *Central European Geology*, 53, 311–342, <https://doi.org/10.1556/CEuGeol.53.2010.4.1>

Géczy, B. 1984. Provincialism of Jurassic ammonites, examples from Hungarian faunas. *Acta Geologica Hungarica*, 27, 379–389.

Géczy, B. 1985. Toarci Amonites zónák a Gerecse hegységben. *Földtani Közlöny*, 115, 363–368.

Gröcke, D.R., Hori, R.S., Trabucho-Alexandre, J., Kemp, D.B. and Schwark, L. 2011. An open ocean record of

the Toarcian oceanic anoxic event. *Solid Earth*, 2, 245–257, <https://doi.org/10.5194/se-2-245-2011>

Haas, J. 2012. Influence of global, regional, and local factors on the genesis of the Jurassic manganese ore formation in the Transdanubian Range, Hungary. *Ore Geology Reviews*, 47, 77–86, <https://doi.org/10.1016/j.oregeorev.2011.08.006>

Haq, B.U. 2018. Jurassic sea-level variations: a reappraisal. *GSA Today*, 28, 4–10, <https://doi.org/10.1130/GSATG359A.1>

Häusler, H., Plašienka, D. and Polák, M. 1993. Comparison of Mesozoic successions in the Central Eastern Alps and the Central Western Carpathians. *Jahrbuch der Geologischen Bundesanstalt*, 136, 715–739.

Hermoso, M., Le Callonnec, L., Minoletti, F., Renard, M. and Hesselbo, S.P. 2009. Expression of the Early Toarcian negative carbon-isotope excursion in separated carbonate microfractions (Jurassic, Paris Basin). *Earth and Planetary Science Letters*, 277, 194–203, <https://doi.org/10.1016/j.epsl.2008.10.013>

Hermoso, M., Minoletti, F., Rickaby, R.E., Hesselbo, S.P., Baudin, F. and Jenkyns, H.C. 2012. Dynamics of a stepped carbon-isotope excursion: ultra high-resolution study of Early Toarcian environmental change. *Earth and Planetary Science Letters*, 319, 45–54, <https://doi.org/10.1016/j.epsl.2011.12.021>

Hesselbo, S.P. and Pienkowski, G. 2011. Stepwise atmospheric carbon-isotope excursion during the Toarcian oceanic anoxic event (Early Jurassic, Polish Basin). *Earth and Planetary Science Letters*, 301, 365–372, <https://doi.org/10.1016/j.epsl.2010.11.021>

Hesselbo, S.P., Gröcke, D.R., Jenkyns, H.C., Bjerrum, C.J., Farrimond, P., Bell, H.S.M. and Green, O.R. 2000. Massive dissociation of gas hydrate during a Jurassic oceanic anoxic event. *Nature*, 406, 392–395, <https://doi.org/10.1038/35019044>

Hesselbo, S.P., Jenkyns, H.C., Duarte, L.V. and Oliveira, L.C. 2007. Carbon-isotope record of the Early Jurassic (Toarcian) Oceanic Anoxic Event from fossil wood and marine carbonate (Lusitanian Basin, Portugal). *Earth and Planetary Science Letters*, 253, 455–470, <https://doi.org/10.1016/j.epsl.2006.11.009>

Huang, C. and Hesselbo, S.P. 2014. Pacing of the Toarcian Oceanic Anoxic Event (Early Jurassic) from astronomical correlation of marine sections. *Gondwana Research*, 25, 1348–1356, <https://doi.org/10.1016/j.gr.2013.06.023>

Izumi, K., Miyaji, T. and Tanabe, K. 2012. Early Toarcian (Early Jurassic) oceanic anoxic event recorded in the shelf deposits in the northwestern Panthalassa: evidence from the Nishinakayama Formation in the Toyora area, west Japan. *Palaeogeography, Palaeoclimatology, Palaeoecology*, 315, 100–108, <https://doi.org/10.1016/j.palaeo.2011.11.016>

Jenkyns, H.C. 1988. The early Toarcian (Jurassic) anoxic event – stratigraphic, sedimentary, and geochemical evidence. *American Journal of Science*, 288, 101–151, <https://doi.org/10.2475/ajs.288.2.101>

Jenkyns, H.C. 2010. Geochemistry of oceanic anoxic events. *Geochemistry, Geophysics, Geosystems*, 11, 1–30, <https://doi.org/10.1029/2009GC002788>

Jenkyns, H.C. and Clayton, C.J. 1986. Black shales and carbon isotopes in pelagic sediments from the Tethyan Lower Jurassic. *Sedimentology*, 33, 87–106, <https://doi.org/10.1111/j.1365-3091.1986.tb00746.x>

Jenkyns, H.C., Géczy, B. and Marshall, J.D. 1991. Jurassic manganese carbonates of central Europe and the early Toarcian anoxic event. *The Journal of Geology*, 99, 137–149, <https://doi.org/10.1086/629481>

Kafousia, N., Karakitsios, V., Jenkyns, H.C. and Mattioli, E. 2011. A global event with a regional character: the Early Toarcian Oceanic Anoxic Event in the Pindos Ocean (northern Peloponnese, Greece). *Geological Magazine*, 148, 619–631, <https://doi.org/10.1017/S0016756811000082>

Kemp, D.B., Coe, A.L., Cohen, A.S. and Schwark, L. 2005. Astronomical pacing of methane release in the Early Jurassic period. *Nature*, 437, 396–399, <https://doi.org/10.1038/nature04037>

Kemp, D.B., Selby, D. and Izumi, K. 2020. Direct coupling between carbon release and weathering during the Toarcian oceanic anoxic event. *Geology*, 48, 976–980, <https://doi.org/10.1130/g47509.1>

Knauth, L.P. and Kennedy, M.J. 2009. The late Precambrian greening of the Earth. *Nature*, 460, 728–732, <https://doi.org/10.1038/nature08213>

Konda, J. 1986. Gerecse, Süttő, Kisgerescei kőfejtő (Kisgeresce quarry, Süttő, Gerecse), Magyar Állami Földtani Intézet (Hungarian Geological Institute), Magyarország geológiai alapszelvényei (Geological Reference Sections of Hungary).

Konda, J. 1988. Gerecse, Lábatlan, Tölgyhádi kőfejtő (Tölgyhát quarry, Lábatlan, Gerecse), Magyar Állami Földtani Intézet (Hungarian Geological Institute), Magyarország geológiai alapszelvényei (Geological Reference Sections of Hungary). Kovács, Z. 2012. Lower Toarcian Ammonitida fauna and biostratigraphy of the Gerecse Mountains (Hungary). *Fragmenta Palaeontologica Hungarica*, 29, 1–48.

Krencker, F.N., Lindström, S. and Bodin, S. 2019. A major sea-level drop briefly precedes the Toarcian oceanic anoxic event: implication for Early Jurassic climate and carbon cycle. *Scientific Reports*, 9, 12518, <https://doi.org/10.1038/s41598-019-48956-x>

Krencker, F.N., Fantasia, A., Danisch, J., Martindale, R., Kabiri, L., El Ouali, M. and Bodin, S. 2020. Two-phased collapse of the shallow-water carbonate factory during the late Pliensbachian–Toarcian driven by changing climate and enhanced continental weathering in the Northwestern Gondwana Margin. *Earth-Science Reviews*, 208, 103254, <https://doi.org/10.1016/j.earscirev.2020.103254>

Küspert, W. 1982. Environmental changes during oil shale deposition as deduced from stable isotope ratios. In: Einsele, G. and Seilacher, A. (eds) *Cyclic and Event Stratification*. Springer, 482–501, [https://doi.org/10.1007/978-3-642-75829-4\\_36](https://doi.org/10.1007/978-3-642-75829-4_36)

Léonide, P., Floquet, M., Durllet, C., Baudin, F., Pittet, B. and Lécuyer, C. 2012. Drowning of a carbonate platform as a precursor stage of the Early Toarcian global anoxic event (Southern Provence sub-Basin, south-east France). *Sedimentology*, 59, 156–184, <https://doi.org/>



[10.1111/j.1365-3091.2010.01221.x](https://doi.org/10.1111/j.1365-3091.2010.01221.x)

- Littler, K., Hesselbo, S.P. and Jenkyns, H.C. 2010. A carbon-isotope perturbation at the Pliensbachian–Toarcian boundary: evidence from the Lias Group, NE England. *Geological Magazine*, 147, 181–192, <https://doi.org/10.1017/S0016756809990458>
- Lohmann, K.C. 1988. Geochemical patterns of meteoric diagenetic systems and their application to studies of paleokarst. In: James, N.P. and Choquette, P.W. (eds) *Paleokarst*. Springer, 58–80, [https://doi.org/10.1007/978-1-4612-3748-8\\_3](https://doi.org/10.1007/978-1-4612-3748-8_3)
- Marquart, R.G., Katsnelson, I., Milne, G.W.A., Heller, S.R., Johnson, G.G. and Jenkyns, R. 1979. A searchmatch system for X-ray powder diffraction data. *Journal of Applied Crystallography*, 12, 629–634, <https://doi.org/10.1107/S0021889879013522>
- Mattioli, E. and Erba, E. 1999. Biostratigraphic synthesis of calcareous nannofossil events in the Tethyan Jurassic. *Rivista Italiana di Paleontologia e Stratigrafia*, 105, 343–376.
- Mattioli, E., Pittet, B., Petitpierre, L. and Mailliot, S. 2009. Dramatic decrease of pelagic carbonate production by nannoplankton across the Early Toarcian anoxic event (T-OAE). *Global and Planetary Change*, 65, 134–145, <https://doi.org/10.1016/j.gloplacha.2008.10.018>
- McElwain, J.C., Wade-Murphy, J. and Hesselbo, S.P. 2005. Changes in carbon dioxide during an oceanic anoxic event linked to intrusion into Gondwana coals. *Nature*, 435, 479–482, <https://doi.org/10.1038/nature03618>
- Meister, C., Schirolli, P. and Dommergues, J.-L. 2017. Early Jurassic (Sinemurian to basal Toarcian) ammonites of the Brescian Prealps (Southern Alps, Italy). *Rivista Italiana di Paleontologia e Stratigrafia*, 123, 79–148, <https://doi.org/10.13130/2039-4942/8072>
- Müller, T., Price, G.D. et al. 2017. New multiproxy record of the Jenkyns Event (also known as the Toarcian Oceanic Anoxic Event) from the Mecsek Mountains (Hungary): differences, duration and drivers. *Sedimentology*, 64, 66–86, <https://doi.org/10.1111/sed.12332>
- Müller, T., Jurikova, H. et al. 2020a. Ocean acidification during the early Toarcian extinction event: evidence from boron isotopes in brachiopods. *Geology*, 48, 1184–1188, <https://doi.org/10.1130/G47781.1>
- Müller, T., Karancz, S. et al. 2020b. Assessing anoxia, recovery and carbonate production setback in a hemipelagic Tethyan basin during the Toarcian Oceanic Anoxic Event (Western Carpathians). *Global and Planetary Change*, 195, 103366, <https://doi.org/10.1016/j.gloplacha.2020.103366>
- Neumeister, S., Gratzner, R., Algeo, T.J., Bechtel, A., Gawlick, H.J., Newton, R.J. and Sachsenhofer, R.F. 2015. Oceanic response to Pliensbachian and Toarcian magmatic events: implications from an organic-rich basinal succession in the NW Tethys. *Global and Planetary Change*, 126, 62–83, <https://doi.org/10.1016/j.gloplacha.2015.01.007>
- Pálffy, J. and Smith, P.L. 2000. Synchrony between Early Jurassic extinction, oceanic anoxic event, and the Karoo–Ferrar flood basalt volcanism. *Geology*, 28, 747–750.
- Pearce, C.R., Cohen, A.S., Coe, A.L. and Burton, K.W. 2008. Molybdenum isotope evidence for global ocean anoxia coupled with perturbations to the carbon cycle during the Early Jurassic. *Geology*, 36, 231–234, <https://doi.org/10.1130/G24446a.1>
- Percival, L.M., Cohen, A.S. et al. 2016. Osmium isotope evidence for two pulses of increased continental weathering linked to Early Jurassic volcanism and climate change. *Geology*, 44, 759–762, <https://doi.org/10.1130/G37997.1>
- Pittet, B., Suan, G., Lenoir, F., Duarte, L.V. and Mattioli, E. 2014. Carbon isotope evidence for sedimentary discontinuities in the lower Toarcian of the Lusitanian Basin (Portugal): sea level changes at the onset of the Oceanic Anoxic Event. *Sedimentary Geology*, 303, 1–14, <https://doi.org/10.1016/j.sedgeo.2014.01.001>
- Polgári, M., Szabó, Z. and Szederkényi, T. (eds) 2000. *Mangánércsek Magyarországon – Grasselly Gyula akadémikus emlékére* (Manganese Ores in Hungary – Tribute to Professor Gyula Grasselly). Juhász Nyomda. (In Hungarian.)
- Polgári, M., Hein, J.R. et al. 2016. Mineral and chemostratigraphy of a Toarcian black shale hosting Mn-carbonate microbialites (Úrkút, Hungary). *Palaeogeography, Palaeoclimatology, Palaeoecology*, 459, 99–120, <https://doi.org/10.1016/j.palaeo.2016.06.030>
- Raucsik, B. and Varga, A. 2008. Climato-environmental controls on clay mineralogy of the Hettangian–Bajocian successions of the Mecsek Mountains, Hungary: an evidence for extreme continental weathering during the early Toarcian oceanic anoxic event. *Palaeogeography, Palaeoclimatology, Palaeoecology*, 265, 1–13, <https://doi.org/10.1016/j.palaeo.2008.02.004>
- Reolid, M., Mattioli, E., Duarte, L. and Marok, A. 2020. The Toarcian Oceanic Anoxic Event and the Jenkyns Event (IGCP-655 final report). *Episodes*, 43, 833–844, <https://doi.org/10.18814/epiiugs/2020/020051>
- Rocha, R.B., Mattioli, E. et al. 2016. Base of the Toarcian Stage of the Lower Jurassic defined by the Global Boundary Stratotype Section and Point (GSSP) at the Peniche section (Portugal). *Episodes*, 39, 460–481, <https://doi.org/10.18814/epiiugs/2016/v39i3/99741>
- Rosales, I., Quesada, S. and Robles, S. 2001. Primary and diagenetic isotopic signals in fossils and hemipelagic carbonates: the Lower Jurassic of northern Spain. *Sedimentology*, 48, 1149–1169, <https://doi.org/10.1046/j.1365-3091.2001.00412.x>
- Rosales, I., Barnolas, A., Goy, A., Sevillano, A., Armendáriz, M. and López-García, J.M. 2018. Isotope records (CO–Sr) of late Pliensbachian–early Toarcian environmental perturbations in the westernmost Tethys (Majorca Island, Spain). *Palaeogeography, Palaeoclimatology, Palaeoecology*, 497, 168–185, <https://doi.org/10.1016/j.palaeo.2018.02.016>
- Roth, P.H. 1984. Preservation of calcareous nannofossils and fine-grained carbonate particles in mid-Cretaceous sediments from the southern Angola Basin. In: Hay, W.W., Sibuet, J.C. et al. (eds), *Initial Reports DSDP*, 75, 651–655, <https://doi.org/10.2973/dsdp.proc.75.112.1984>
- Ruebsam, W. and Al-Husseini, M. 2020. Calibrating the Early Toarcian (Early Jurassic) with stratigraphic black holes (SBH). *Gondwana Research*, 82, 317–336, <https://doi.org/10.1016/j.gr.2020.01.011>
- Ruebsam, W., Müller, T., Kovács, J., Pálffy, J. and Schwark, L. 2018. Environmental response to the early Toarcian carbon cycle and climate perturbations in the northeastern part of the West Tethys shelf. *Gondwana Research*, 59, 144–158, <https://doi.org/10.1016/j.gr.2018.03.013>
- Ruebsam, W., Mayer, B. and Schwark, L. 2019. Cryosphere carbon dynamics control early Toarcian global warming and sea level evolution. *Global and Planetary Change*

Change, 172, 440–453, <https://doi.org/10.1016/j.gloplacha.2018.11.003>

Sasvári, A., Csontos, L. and Palotai, M. 2009. Szerkezetgeológiai megfigyelések a gerecsei Tölgyhát-kőfejtőben (Structural geological observations in Tölgyhát Quarry, Gerece Mts., Hungary). *Földtani Közlöny*, 139, 55–66.

Schobben, M., Ullmann, C.V. et al. 2016. Discerning primary v. diagenetic signals in carbonate carbon and oxygen isotope records: an example from the Permian–Triassic boundary of Iran. *Chemical Geology*, 422, 94–107, <https://doi.org/10.1016/j.chemgeo.2015.12.013>

Schouten, S., van Kaam-Peters, H.M., Rijpstra, W.I.C., Schoell, M. and Damste, J.S.S. 2000. Effects of an oceanic anoxic event on the stable carbon isotopic composition of early Toarcian carbon. *American Journal of Science*, 300, 1–22, <https://doi.org/10.2475/ajs.300.1.1>

Silva, R.L., Duarte, L.V., Comas-Rengifo, M.J., MendonçaFilho, J.G. and Azerêdo, A.C. 2011. Update of the carbon and oxygen isotopic records of the Early–Late Pliensbachian (Early Jurassic, ~187 Ma): insights from the organic-rich hemipelagic series of the Lusitanian Basin (Portugal). *Chemical Geology*, 283, 177–184, <https://doi.org/10.1016/j.chemgeo.2011.01.010>

Suan, G., Mattioli, E., Pittet, B., Mailliot, S. and Lécuyer, C. 2008a. Evidence for major environmental perturbation prior to and during the Toarcian (Early Jurassic) oceanic anoxic event from the Lusitanian Basin, Portugal. *Paleoceanography*, 23, 1–14, <https://doi.org/10.1029/2007pa001459>

Suan, G., Pittet, B., Bour, I., Mattioli, E. and Duarte, L.V. 2008b. Duration of the Early Toarcian carbon isotope excursion deduced from spectral analysis: consequence for its possible causes. *Earth and Planetary Science Letters*, 267, 666–679, <https://doi.org/10.1016/j.epsl.2007.12.017>

Suan, G., Mattioli, E. et al. 2010. Secular environmental precursors to Early Toarcian (Jurassic) extreme climate changes. *Earth and Planetary Science Letters*, 290, 448–458, <https://doi.org/10.1016/j.epsl.2009.12.047>

Suan, G., Nikitenko, B.L. et al. 2011. Polar record of Early Jurassic massive carbon injection. *Earth and Planetary Science Letters*, 312, 102–113, <https://doi.org/10.1016/j.epsl.2011.09.050>

Suan, G., van de Schootbrugge, B., Adatte, T., Fiebig, J. and Oschmann, W. 2015. Calibrating the magnitude of the Toarcian carbon cycle perturbation. *Paleoceanography*, 30, 495–509, <https://doi.org/10.1002/2014PA002758>

Suan, G., Schlögl, J. and Mattioli, E. 2016. Bio- and chemostratigraphy of the Toarcian organic-rich deposits of some key successions of the Alpine Tethys. *Newsletters on Stratigraphy*, 49, 401–419, <https://doi.org/10.1127/nos/2016/0078>

Suan, G., Schöhlhorn, I., Schlögl, J., Segit, T., Mattioli, E., Lécuyer, C. and Fourrel, F. 2018. Euxinic conditions and high sulfur burial near the European shelf margin (Pieniny Klippen Belt, Slovakia) during the Toarcian oceanic anoxic event. *Global and Planetary Change*, 170, 246–259, <https://doi.org/10.1016/j.gloplacha.2018.09.003>

Svensen, H., Planke, S., Chevallier, L., Mørch-Sørensen, A., Corfu, F. and Jamveit, B. 2007. Hydrothermal venting of greenhouse gases triggering Early Jurassic global warming. *Earth and Planetary Science Letters*, 256, 554–566, <https://doi.org/10.1016/j.epsl.2007.02.013>

Them, I., T.R., Gill, B.C. et al. 2017. High-resolution carbon isotope records of the Toarcian Oceanic Anoxic Event (Early Jurassic) from North America and implications for the global drivers of the Toarcian carbon cycle. *Earth and Planetary Science Letters*, 459, 118–126, <https://doi.org/10.1016/j.epsl.2016.11.021>

Them, T.R., Gill, B.C. et al. 2018. Thallium isotopes reveal protracted anoxia during the Toarcian (Early Jurassic) associated with volcanism, carbon burial, and mass extinction. *Proceedings of the National Academy of Sciences*, 115, 6596–6601, <https://doi.org/10.1073/pnas.1803478115>

Thierry, J. and Barrier, E. 2000. Middle Toarcian. In: Dercourt, J., Gaetani, M. et al. (eds) *Atlas Peri-Tethys, Paleogeographic Maps. CCGM/CGMW*, Map 8.

Trecall, A., Spangenberg, J., Adatte, T., Föllmi, K.B. and Parente, M. 2012. Carbonate platform evidence of ocean acidification at the onset of the early Toarcian oceanic anoxic event. *Earth and Planetary Science Letters*, 357, 214–225, <https://doi.org/10.1016/j.epsl.2012.09.043>

Ullmann, C.V., Thibault, N., Ruhl, M., Hesselbo, S.P. and Korte, C. 2014. Effect of a Jurassic oceanic anoxic event on belemnite ecology and evolution. *Proceedings of the National Academy of Sciences*, 111, 10073–10076, <https://doi.org/10.1073/pnas.1320156111>

van Breugel, Y., Baas, M., Schouten, S., Mattioli, E. and Sinninghe-Damste, J.S. 2006. Isorenieratane record in black shales from the Paris Basin, France: constraints on recycling of respired CO<sub>2</sub> as a mechanism for negative carbon isotope shifts during the Toarcian oceanic anoxic event. *Paleoceanography*, 21, PA4220, <https://doi.org/10.1029/2006PA001305>

van de Schootbrugge, B., Bailey, T.R. et al. 2005. Early Jurassic climate change and the radiation of organic-walled phytoplankton in the Tethys Ocean. *Paleobiology*, 31, 73–97, [https://doi.org/10.1666/0094-8373\(2005\)031%3C0073:ejccat%3E2.0.co;2](https://doi.org/10.1666/0094-8373(2005)031%3C0073:ejccat%3E2.0.co;2)

Vetö, I., Demény, A., Hertelendi, E. and Hetényi, M. 1997. Estimation of primary productivity in the Toarcian Tethys – a novel approach based on TOC, reduced sulphur and manganese contents. *Palaeogeography, Palaeoclimatology, Palaeoecology*, 132, 355–371, [https://doi.org/10.1016/s0031-0182\(97\)00053-9](https://doi.org/10.1016/s0031-0182(97)00053-9)

Vörös, A. and Galács, A. 1998. Jurassic palaeogeography of the Transdanubian Central Range (Hungary). *Rivista Italiana di Paleontologia e Stratigrafia*, 104, 69–84.

Wohlwend, S., Hart, M.B. and Weissert, H. 2016. Chemostratigraphy of the Upper Albian to mid-Turonian Natih Formation (Oman) – how authigenic carbonate changes a global pattern. *The Depositional Record*, 2, 97–117, <https://doi.org/10.1002/dep2.15>

Xu, W., Ruhl, M. et al. 2017. Carbon sequestration in an expanded lake system during the Toarcian oceanic anoxic event. *Nature Geoscience*, 10, 129–134, <https://doi.org/10.1038/ngeo2871>

Xu, W., Ruhl, M. et al. 2018. Evolution of the Toarcian (Early Jurassic) carbon-cycle and global climatic controls on local sedimentary processes (Cardigan Bay Basin, UK). *Earth and Planetary Science Letters*, 484, 396–411, <https://doi.org/10.1016/j.epsl.2017.12.037>